THE GEOLOGY OF ROUND MOUNTAIN, A BIMODAL VOLCANIC FIELD IN NORTHWEST ARIZONA

by

MARK M. BUSH

A thesis submitted to the faculty of the Gradaute School of the State University of New York at Buffalo in partial fulfillment of the requirements for the degree of Master of Arts

June, 1986

ABSTRACT

Round Mountain is a prominent rhyolite dome of late Tertiary age located in northwestern Arizona. The dome has a local relief of 268 m and is approximately 2.1 km in diameter at its base.

Round Mountain developed through both endogenous and exogenous phases. Initial stages of dome development were characterized by endogenous growth and the formation of rhyolite breccia units which constitute approximately 30-40 percent of the total erupted rhyolite. Later volcanic phases involved the eruption of 4 major rhyolite flows that cap the dome.

The Round Mountain volcanic field is strongly bimodal, consisting of high-K rhyolite and alkali olivine basalt with 76.3 and 49.5 mean SiO_2 percentages respectively. The rhyolites are composed of approximately 90 percent glass with dominant phenocrystalline phases of sanidine and high-temperature oligoclase.

Emplacement of Round Mountain is believed to have been initiated by the intrusion into the upper crust of hot basaltic magma that had migrated preferentially along major crustal fracture zones. Rhyolite magma was generated by the partial melting of a granitic crust and later emplaced along surficial fracture zones.

ACKNOWLEDGEMENTS

I would like to sincerely thank Dr. John S. King, my major advisor, for his greatly appreciated suggestions and encouragement concerning the preparation of this thesis. His informative discussions and comments have lead not only to the completion of this study, but also to a lasting friendship.

I would also like to thank Dr. John Fountain and Dr. Charles Clemency for their critical review of this thesis. Their comments and suggestions have significantly improved the content of this text.

My most heartfelt appreciation goes to my parents, George and Pauline, for their support and encouragement. I am grateful for thier patience and understanding during my never ending saga of higher education.

An expression of gratitude is also given to L. David Nealey at the USGS, Flagstaff for his willingness to aid me in my research.

Lastly, I would like to thank Exxon for offering me an ideal job which provided a great deal of incentive to complete this study.

The majority of this research was funded under National Aeronautics and Space Administration Planetary Grant NGR 330-151-08 awarded to Dr. John S. King. Minor funding was also made possible from a grant given by the Graduate Student Association.

TABLE OF CONTENTS

LIST OF FIGURES

LIST OF PLATES

INTRODUCTION

Round Mountain is a distinctive rhyolitic dome positioned on the Colorado Plateau in northwestern Arizona. It is located approximately 100 km west of Flagstaff and 19 km northeast of Seligman, Arizona. Round Mountain rises to a maximum elevation of 2163 m above sea level and has a local relief of 268 meters.

The strongly bimodal Round Mountain volcanic field, containing high-K rhyolites and alkali olivine basalts, has received no previous investigative attention. The Mount Floyd volcanic field immediately south of Round Mountain, has been intensively studied by Nealey (1980). Potassium-argon data from the volcanics in the northern sector of the Mount Floyd field indicate an age of 2.7 +/- 0.7 m.y. (Nealey, 1980). Based on volcanic stratigraphy, the Round Mountain volcanics are considered to be more recent.

PURPOSE OF STUDY

The purpose of this study was to investigate the geology of Round Mountain. More specifically, this research was aimed at providing a detailed description of the volcanic morphology and processes which were involved in the formation of Round Mountain. This was accomplished by

developing a geologic map of the study area in conjunction with petrographic examination and geochemical analysis of volcanic rock samples collected during the mapping. An additional aspect of this study involved the investigation of planetary analogs of Round Mountain to correlate possible origins of similar morphologic features of martian and lunar terrains.

The preparation of the geologic map (plate 1) involved field mapping of approximately 21 km^2 on an enlarged 1973 USGS Mount Floyd 7.5' topographic quadrangle. Contacts of the volcanic units were verified using 1972 USGS aerial photographs GS-VCZV 1-116, 1-118, and 1-127.

Petrographic thin sections of 43 volcanic rock samples of the study area were prepared and examined. Modal analyses and petrographic descriptions were performed, the results of which are presented in appendices B and C.

Geochemical data of 24 samples from the study area were collected using whole rock x-ray fluorescence methods. The analyses yielded both the major and trace element data, given in appendices D and E.

REGIONAL SETTING

STRUCTURE

Northwestern Arizona is a part of the southwestern portion of the Colorado Plateau physiographic province. This section of the Colorado Plateau is considered to be composed of large structural blocks or regions whose boundaries are delineated by north-northeast and northwest trending faults (Lucchitta, 1974). These structural blocks have a low angle of dip to the northeast.

The major north-northeast trending fault systems of northwestern Arizona are, from east to west: the Oak Creek Canyon system; the Mesa Butte system; the Bright Angel system; and the Sinyala system (Figure 1). The major northwest trending fault systems are, from north to south: the Mormon Ridges system; the Kaibab system; the Cataract Creek system; and the Chino Valley system. These fault systems extend for tens to hundreds of kilometers with displacements which range from hundreds to thousands of meters (Lucchitta, 1974). Most of the faults are high angle dip slip with their downthrown sides to the west (Figure 2).

The Round Mountain, Trinity Mountain, and Howard Hill volcanic complexes lie along the southern projection of the Bright Angel fault system, with the Mount Floyd volcanic center lying directly on the fault trace as shown in figure

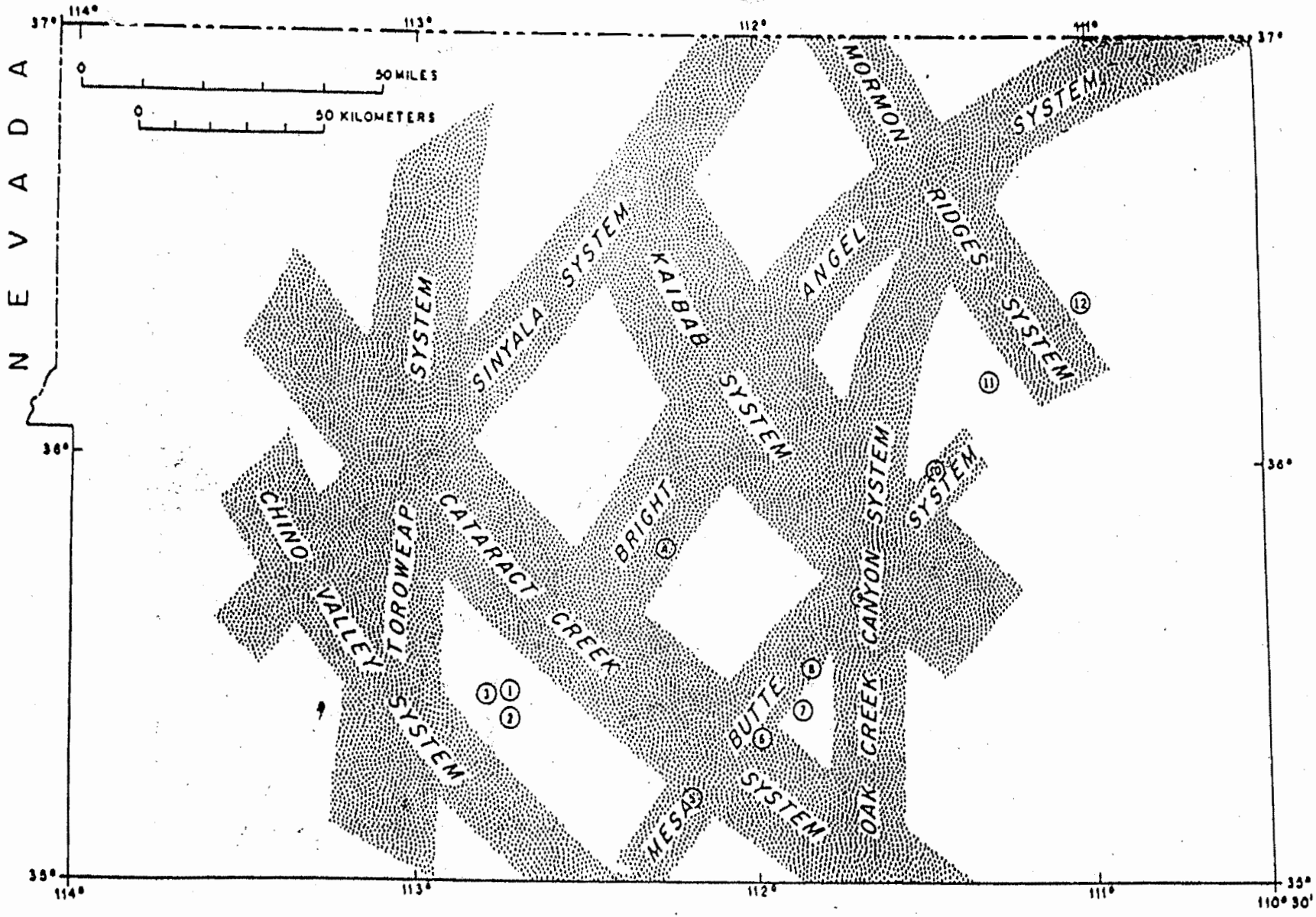

Figure 1 - Major fault systems of northwestern Arizona showing volcanic center locations. Volcanic centers are shown by circles: 1) Round Mtn.; 2) Mount Floyd; 3) Trinity Mtn.; 4) Howard Hill; 5) Bill Williams Mtn.; 6) Sitgreaves Mtn.; 7) Kendrick Peak; 8) Slate Mtn.; 9) Mesa Butte; 10) Shadow Mtn.; 11) Tuba Butte; 12) Wildcat Peak (modified from Shoemaker and others, 1974).

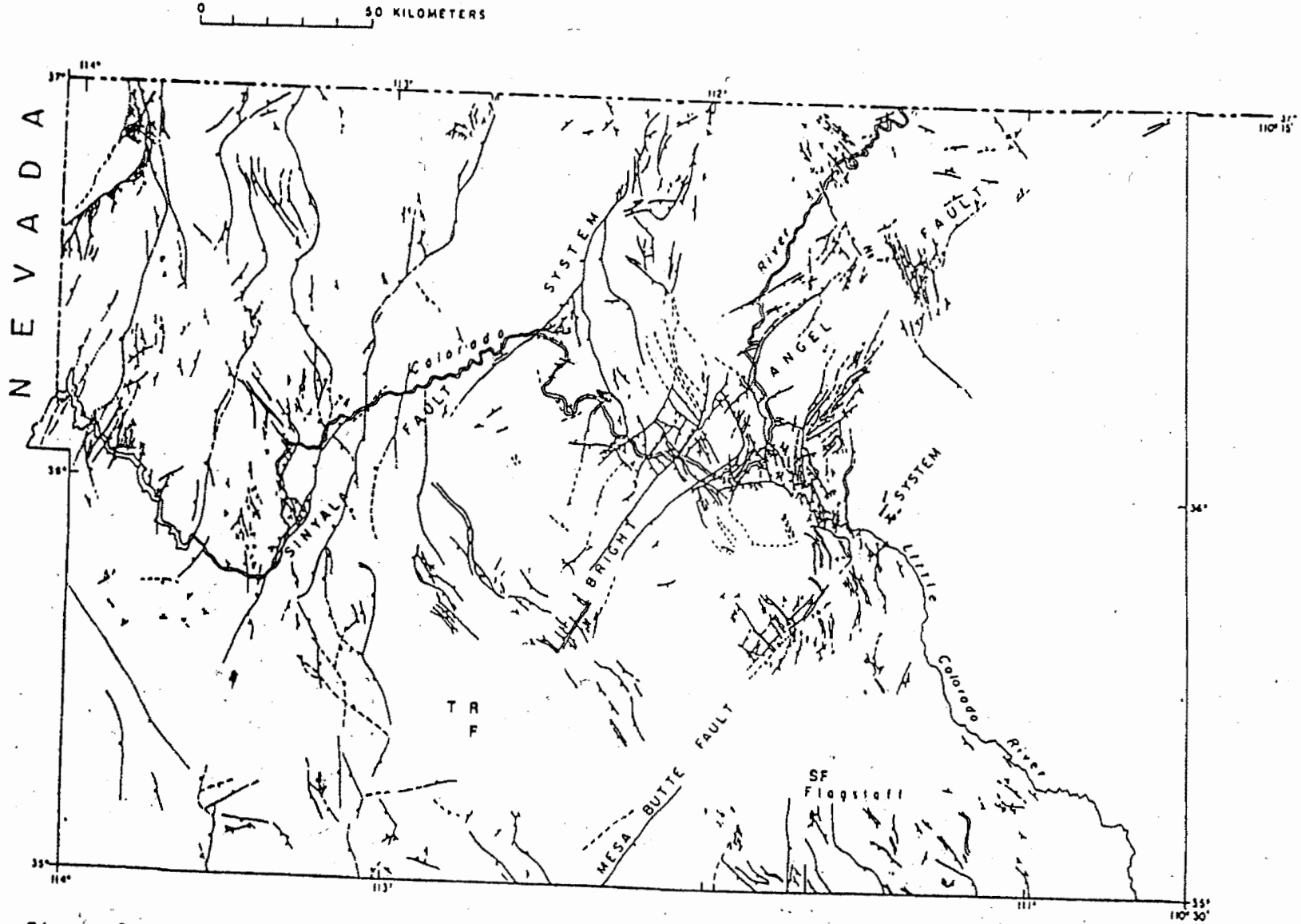

Figure 2 - Composite map of faults in northwestern Arizona the locations of (R)-Round Mtn.; (T)-Trinity Mtn.; (F)-Mount Floyd; and (SF)-San Francisco Mtn. Normal faults are shown with a dot on the downthrown side (after Shoemaker and others, 1974).

1. These three volcanic centers are bounded to the north and south by the Cataract Creek and Chino Valley fault systems.

Locations of many other volcanic centers located near the map area also correlate with major fault systems. The Cenozoic volcanic centers of : Bill Williams Mountain, Sitgreaves Mountain, Kendrick Peak, Slate Mountain, Mesa Butte, Shadow Mountain, Tuba Butte, and Wildcat Peak all lie on, or along projections of, the Mesa Butte fault system.

In northwestern Arizona, the Colorado Plateau Province and the Basin and Range Province which adjoins it to the south have distinctive structural, geophysical, volcanic, crustal, and physiographic properties which distinguish them. The width of the physiographic boundary between these two provinces varies, but is generally about 10 kilometers in northwestern Arizona. By contrast the geophysical boundary in this region places constraints which limit the width to approximately 80 kilometers (Shuey et al, 1973). Lucchitta (1974) concluded that the parallelism of certain structural features which cross the boundary between the Colorado Plateau and the Basin and Range in northwestern Arizona could only be the result of common stress fields being applied to both provinces. The fact that the structural deformation regimes between the provinces is different is a function of the crustal properties, with the Colorado Plateau having a more competent and thick crust.

The Colorado Plateau in this region is characterized by

a 37-42 kilometer thick crust. There are numerous southeast-northwest trending monoclines whose steep limbs dip to the northeast. Volcanism on the Plateau in this region is Plio-Pleistocene and mid-Tertiary with eruptive locations that are closely associated with zones of weakness in the lower crust (Eastwood, 1974). Although the isolation of volcanism may be in part controlled by lower crustal or upper mantle irregularities, it is the upper crustal properties and weakness zones which delimit the locations and style of these faults. These upper crustal faults may modify the final location of the volcanic centers.

REGIONAL GEOPHYSICS

The geophysical signatures of the Colorado Plateau and the Basin and Range are markedly different. Basin and Range crustal thickness is generally considered to be in the order of 30 kilometers in contrast to that of the Colorado Plateau which averages between 37-42 kilometers (Keller et al., 1979). Based on seismic data, Julian (1970) proposed that under the Basin and Range the low velocity zone in the upper mantle is thick and shallow, in contrast to the Colorado Plateau where it is much deeper and not as well developed. This correlates well with the relatively high heat flow values, ranging from 1 to 3 heat flow units, which are characteristic of the Basin and Range (Roy and others,

1968).

Regional Bouguer gravity maps which span the Colorado Plateau - Basin and Range physiographic boundary show a definite change in gravity signatures. There is a decrease from the higher values observed in the Basin and Range to the relatively low values in the Plateau region.

Aeromagnetic data show an anomalous gradient across the boundary between the two provinces with lows over the Basin and Range to the high seen on the Colorado Plateau (Shuey et al, 1973). Residual aeromagnetic maps (Figure 3) compiled by Sauck and Sumner (1971) and modified by Lucchitta (1974) exhibit minor correlation with the inferred locations of ancestral fault systems and their projections in northwest Arizona. The Round Mountain, Mount Floyd, and Trinity Mountain volcanic centers are located in an area yielding residual magnetic intensity values of less than 0 gammas.

Northwestern Arizona can be considered to be an area of active seismicity. Figure 4 (Lucchitta, 1974) shows the plots of 26 recorded earthquakes in the area in the period from 1938 to 1973 and their relationship to the major fault systems of the region. By including the inferred projections of these fault systems, there is solid evidence that these fault systems are currently active.

STRATIGRAPHY

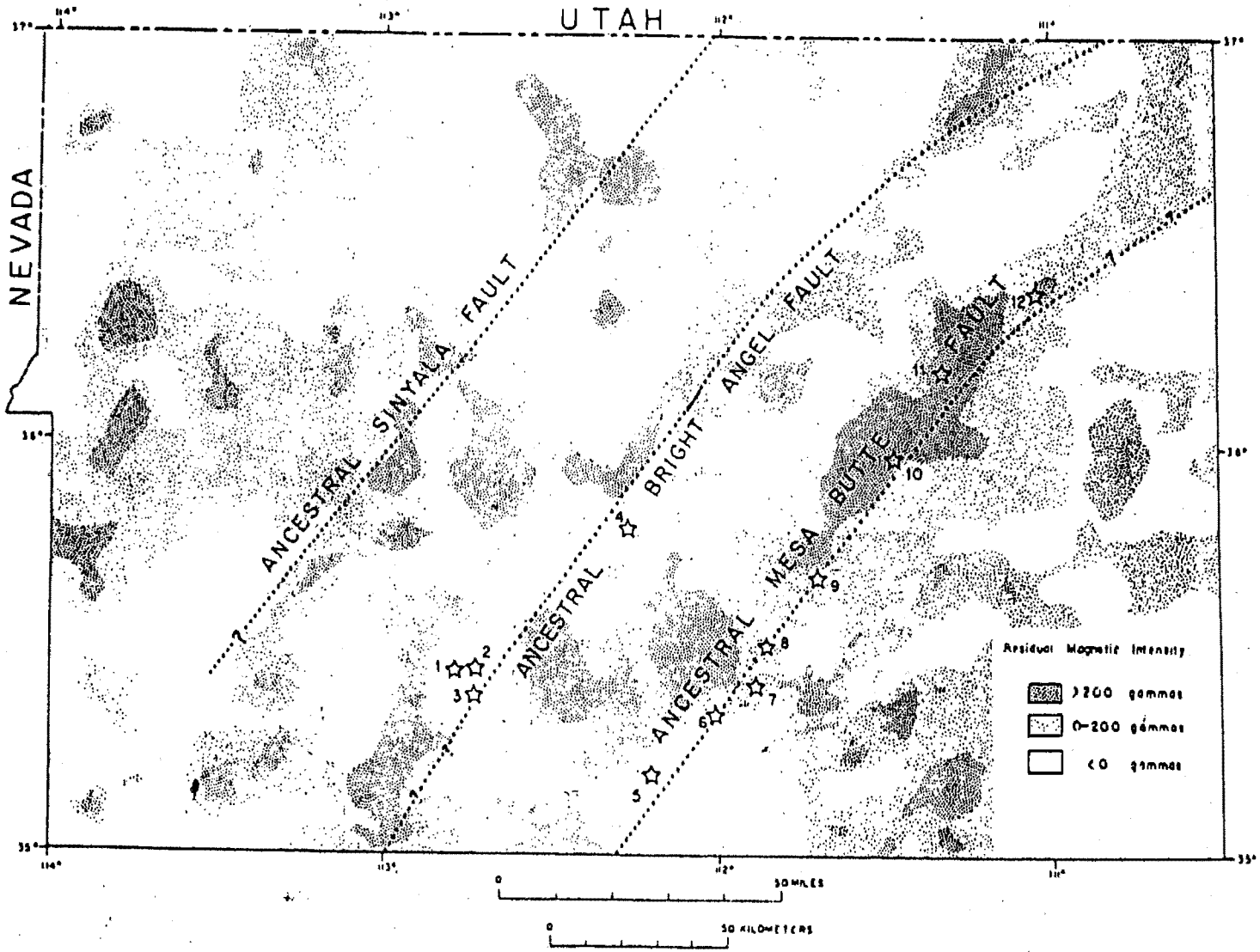

Figure 3. - Residual aeromagnetic map overlain by the traces of ancestral fault systems and related volcanic centers. The volcanic centers shown by stars: 1) Trinity Mtn.; 2) Round Mtn.; 3) Mount Floyd; 4) Howard Hill; 5) Bill Williams Mtn.; 6) Sitgreaves Mtn.; 7) Kendrick Peak; 8) Slate Mtn.; 9) Mesa Butte; 10) Shadow Mtn.; 11) Tuba Butte; 12) Wildcat Peak (after Sauck and Sumner, 1971; Shoemaker, 1974).

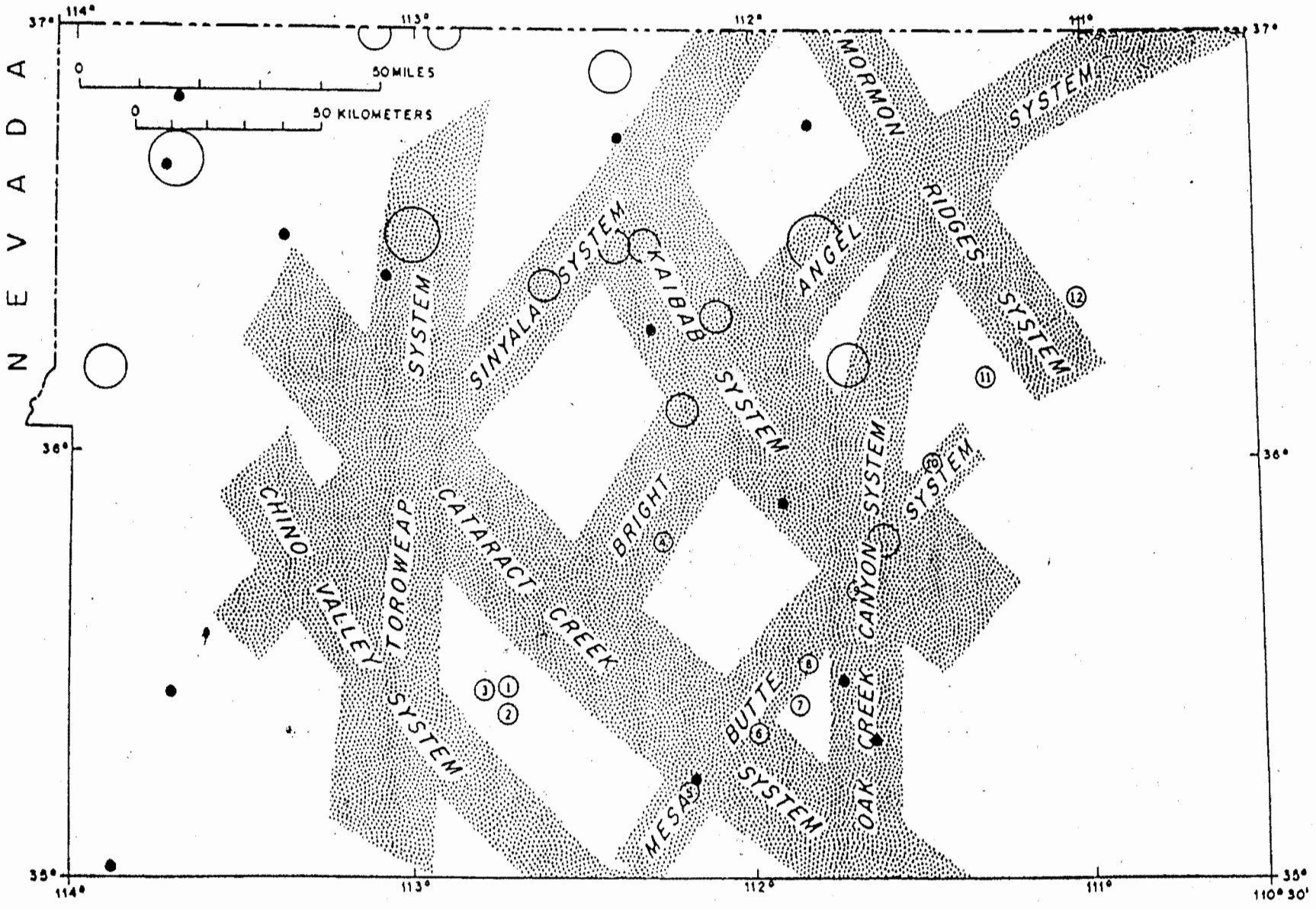

Figure 4. - Earthquake epicenters (dots and open circles) showing their relationship to the major fault systems (after Shoemaker and others, 1974). Volcanic centers are shown by numbered circles: 1) Round Mtn.; 2) Mount Floyd; 3) Trinity Mtn.; 4) Howard Hill; 5) Bill Williams Mtn.; 6) Sitgreaves Mtn.; 7) Kendrick Peak; 8) Slate Mtn.; 9) Mesa Butte; 10) Shadow Mtn.; 11) Tuba Butte; 12) Wildcat Peak

The stratigraphic column for northwest to north-central Arizona is shown in figure 5. The rocks composing the Precambrian basement consist of the Vishnu Group, which are mostly schists and minor amphibolites, the Bass Dolomite, Hakatai Shale, Shinumo Quartzite, and the Dox Sandstone. The Precambrian basement rocks are overlain by essentially horizontal Paleozoic sedimentary units of sandstone, limestone, dolomite, and shale from various eolian, shallow marine, lacustrine, and fluvial environments (Mckee, 1974). In the Chino Valley region immediately to the south of the Round Mountain and Mount Floyd volcanic complexes, the Chino Valley Formation, a sandstone and dolomitic limestone, overlies the Tapeats Sandstone (Hereford, 1975). The Chino Valley Formation is not present in the stratigraphic sequence in the Grand Canyon area. Overlying the Paleozoic rocks is the Moenkopi Formation of Triassic age. This is predominantely a red silty sandstone and is not seen in the Grand Canyon stratigraphic section further to the north.

In some areas of northwest to north-central Arizona, Cenozoic gravels, of early to middle Tertiary age, overlie the Mesozoic and Paleozoic sedimentary formations. These gravels consist of reworked Mesozoic and Paleozoic sediments, along with a significant contribution from crystalline rocks of disputable origin (Young, 1982). It is generally accepted however that these gravels were deposited across the western Coconino Plateau and along the Mogollon

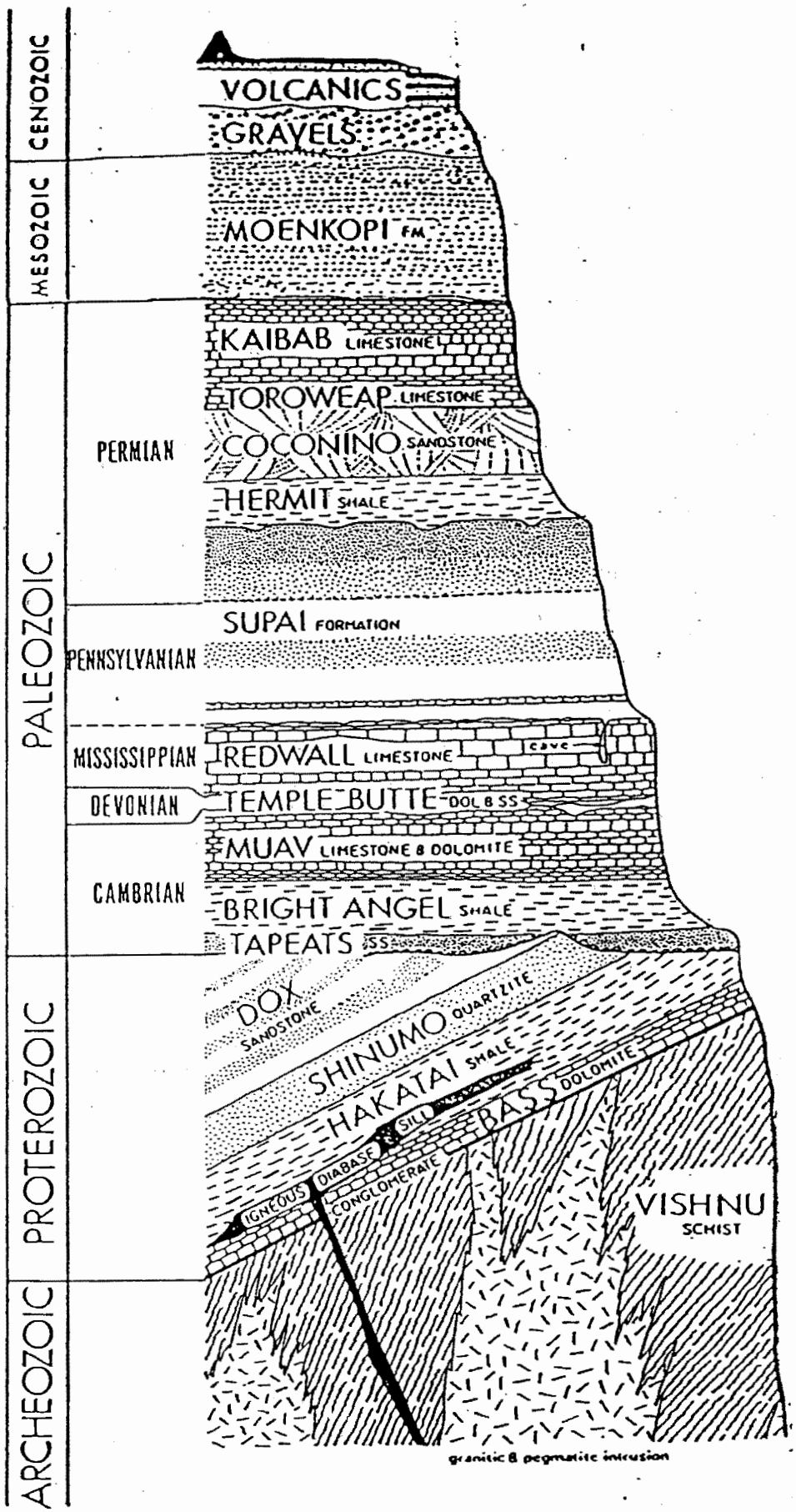

Figure 5. - Stratigraphic column of the rocks of northwestern Arizona (after Breed, 1974).

Rim from sources to the south during early to middle Tertiary (Young, 1982).

Cenozoic volcanics overlie the Tertiary gravels and the Mesozoic and Paleozoic sediments throughout many parts of northwest and north-central Arizona. The observed surficial volcanics are mainly basaltic flows, with some associated intermediate to silicic volcanic centers of dacite, andesite, and rhyolite. These volcanics are of Laramide, middle Tertiary, and Plio-Pleistocene age (Eastwood, 1974).

VOLCANICS

The southwestern United States was volcanically active during three distinctive periods from late Mesozoic through the Cenozoic. Damon (1971) has determined the temporal distributions for the magmatic activity from radiometric data. The first episode is of Laramide age starting 80 m.y. ago and continuing for about 35 m.y.; the second episode was mid-Tertiary in age and ranged from 40 to 10 m.y. ago, while the third major eruptive episode occured in the last 10 m.y., and is dominantely Plio-Pleistocene (Damon, 1971; Eastwood , 1974).

The late Cenozoic igneous suites of the southwestern United States are predominantely basaltic in nature. These lavas were erupted either as basaltic fields, alkalic igneous series derived from alkali basalt, or as bimodal

assemblages consisting of basalt and silica-rich rhyolite (Christiansen and Lipman, 1972). Along the southern margin of the Colorado Plateau, Eastwood (1974) classified the mid-Tertiary volcanism as mainly calc-alkalic with alkaline affinities. Based on petrographic and geochemical data, the volcanic rocks of Plio-Pleistocene age along the southern Colorado Plateau are predominantely alkaline with evidence for a subalkaline affinity (Eastwood, 1974).

These late Cenozoic volcanics are believed to have derived by partial melting from a broad depth interval of the mantle and have been modified by crystal fractionation of olivine, plagioclase, and clinopyroxene during their ascent to the surface (Best and Brimhall, 1974). Damon (1971) commented that the mid-Tertiary and Plio-Pleistocene magmas had fundamentally different source regions. Based on data from Laughlin and others (1972) and Leeman (1974), the strontium 87/86 ratios for mid-Tertiary volcanic rocks are higher relative to those of Plio-Pleistocene age. This may reflect a substantial degree of crustal contamination for the rocks of mid-Tertiary age, with little to no contamination of the Plio-Pleistocene volcanics (Eastwood, 1974; Leeman, 1974).

The San Francisco volcanic field borders the Round Mountain and Mount Floyd volcanic complexes to the east. Situated on the southern edge of the Colorado Plateau, the San Francisco volcanic field is of late Tertiary, and

Quaternary age (Moore and others, 1976). Rocks of the San Francisco complex have been dated by Damon and Leventhal (1974), and Smiley (1958), and show ages ranging from 10 m.y. to 1000 years. The San Francisco volcanic field has an areal extent of more than 5,000 square kilometers. It is composed of numerous basaltic, intermediate, and silicic volcanic centers which are genetically related (Moore and others, 1976).

Based on geochemical and petrographic data, the basic volcanic rocks of the San Francisco field are considered to be alkaline (Hunt, 1956; Eastwood, 1974; Moore and others, 1976) and the chemically intermediate volcanic rocks are found to have a subalkaline affinity (Wenrich-Verbeek and Thornton, 1974). Alkali-olivine basalt is by far the most voluminous rock type in the volcanic field. The San Francisco volcanic field contains alkali-olivine basalts, high-alumina alkali basalts, andesites, dacites, rhyodacites, and rhyolites (Hunt, 1956; Moore, 1973; Moore and others, 1974; 1976).

Based on Sr 87/86 ratios, the San Francisco volcanics show that they are mantle-derived with only minor crustal contamination (Moore et al., 1974). By examining the geochemical data (Moore et al., 1974) obtained from the volcanic rocks of the northern and eastern areas of the San Francisco field, a full differentiation series from basalt to rhyolite has been demonstrated.

The Mount Floyd volcanic field adjoining Round Mountain to the south is considered to be bimodal, with the occurrence of alkalic basalts and calc-alkalic rhyodacites (Nealey, 1980). The age of the Mount Floyd volcanism has been determined, by potassium-argon data, to be 2.7 +/- 0.7 m.y. (Nealey, 1980). The volcanic complex is composed of basaltic and silicic lava flows, domes, cinder cones, and various pyroclastic deposits (Nealey, 1980). The location of the volcanic centers in the Mount Floyd field appears to be in part controlled by the Bright Angel and Chino Valley fault systems.

BASALTS OF THE ROUND MOUNTAIN VOLCANIC FIELD

General Statement

The basaltic rocks within and surrounding the Round Mountain volcanic field have been classified in this study on the basis of color, texture, mineralogy, geochemistry, and location of their source vents. They were categorized into map units and given informal names by the author. In the following sections each basaltic map unit is briefly described both macro and microscopically. A more detailed petrographic description of specific mineral characteristics is given in Appendix C. Plagioclase compositions were determined either by the Michel-Levy statistical method (Heinrich, 1965) or the Microlite method (Heinrich, 1965). Olivine compositions were determined by optic signs and variation in 2V angles (Poldervaart, 1950). The modal analyses for 13 thin sections of the basalt units are presented in Appendix B.

WILLIAMS BASALT (Twb)

Field Description

This basalt is light to medium gray on a fresh surface and dark reddish-black on weathered surfaces. A weathering rind approximately 5 mm thick is commonly present. Visible phenocrysts of olivine (1-3 mm) and quartz xenocrysts are common. Gas vesicles ranging in size from 1 to 10 mm may

occupy up to 50 percent of any exposed surface. This unit forms high profile dikes which commonly radiate from a central vent. Such dikes are generally massive and blocky but may exhibit some degree of foliation due presumably to pulse emplacement.

Petrographic Textures

The Williams basalt is holocrystalline and contains approximately 60 percent phenocrysts of plagioclase (An_{58}), clinopyroxene (augite), olivine (Fo_{75-88}), and minor opaques. Xenocrysts of quartz are present and have clinopyroxene reaction rims. Plagioclase microlites are subparallel resulting in a pilotaxitic fabric. Plagioclase generally shows a subophitic relationship with clinopyroxene but may also form glomeroporphyritic clots. Alteration is slight with only minor olivine alteration to produce iddingsite and iron staining.

JOSEP BASALT (Tjb)

Field Description

Macroscopically this basalt is dark gray-black on a weathered surface and smooth in appearance. On a fresh surface it is seen to contain approximately 2 percent of phenocrysts of olivine (1-2 mm) that are altered to iddingsite. In hand specimen the Josep basalt is very fine grained and generally shows no vesicles. Minor xenocrysts of quartz are present which have a visible reaction rind.

Spheroidal weathering is common near the source vent. This unit forms low profile flows and dikes. At flow fronts this basalt often exhibits a texture produced by the incorporation of basaltic fragments (figure 6).

Petrographic Textures

Microscopically the Josep basalt is holocrystalline with approximately 20 percent phenocrysts of olivine (Fo_{67}) and clinopyroxene (augite ?). The microlites of plagioclase (An_{50}) which form the groundmass have a pilotaxitic fabric indicative of flow. Trace amounts of quartz xenocrysts are present commonly with a rimming of clinopyroxene. Traces of secondary calcite occur within irregular voids. Clinopyroxene may appear as radiating clusters and commonly contains opaques. Plagioclase and clinopyroxene are subophitic and are occasionally embayed by groundmass.

VERNON BASALT (Tvb)

Field Description

This dark gray, very fine grained basalt forms low profile domes and flows. Very few gas vesicles are present in the matrix in hand specimen. Phenocrysts of olivine are rarely visible and are slightly altered. This unit may exhibit small scale flow foliation but is otherwise blocky in structure. It is generally fresh in appearance with an occasional weathering rind about 2 mm thick.

Petrographic Texture

The Vernon basalt is holocrystalline containing approximately 20 percent phenocrysts of plagioclase (An_{54}), olivine (Fo_{75}), and minor clinopyroxene (augite). The groundmass of plagioclase, clinopyroxene, and opaques exhibits a slight pilotaxitic fabric. There is a minor concentration of opaques in areas with a more well-developed pilotaxitic fabric. The intergranular spaces between plagioclase laths in the groundmass are occupied by discrete crystals of clinopyroxene and olivine. Ophitic opaques and clinopyroxene are present in the corroded cores of plagioclase. Plagioclase and clinopyroxene are generally subophitic.

FIELD DAM BASALT (Tfdb)

Field Description

This very fine grained basalt is light gray on weathered surfaces and medium gray on fresh surfaces. Minor amounts of olivine phenocrysts are visible (about 1 mm in diameter). This unit may exhibit a massive, blocky, platey, or spheroidal appearance. The platey basalt is localized near the vent and is presumed to be a product of cyclical effusion of magma. This basalt generally forms low profile flows with an occasional high standing resistant ridge.

Petrographic Texture

Figure 6 - Basaltic gravel (clast) inclusion within a Josep basalt (Tjb) flow front. Note the differential weathering of the matrix basalt surrounding the clasts.

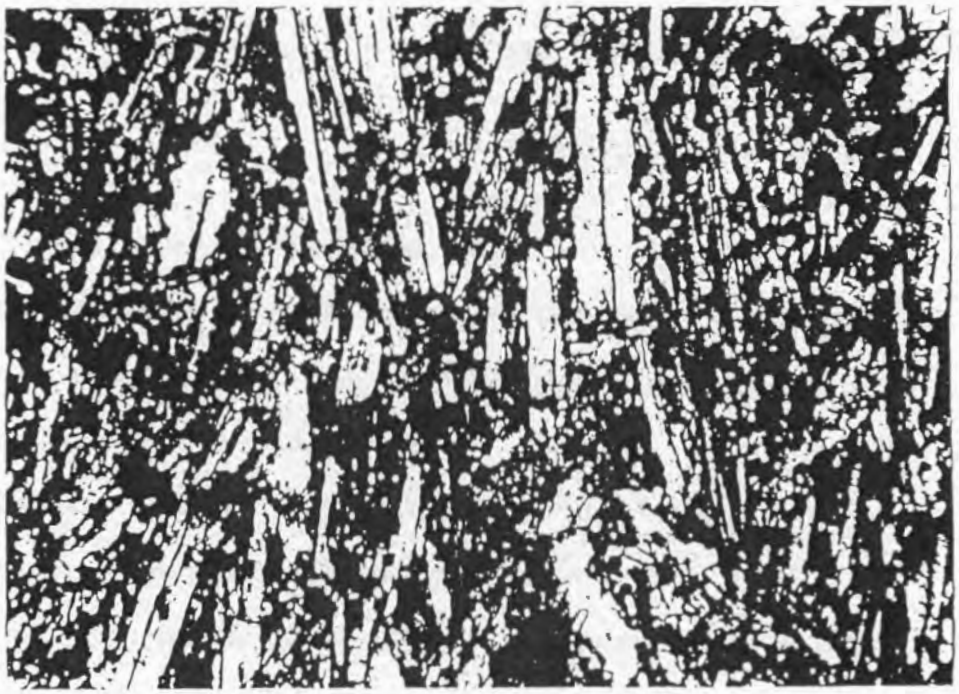

Figure 7 - Photomicrograph (100x) showing the pilotaxitic fabric of the plagioclase microlites in the Basaltic flow (Tbf) unit. The remaining groundmass is composed of clinopyroxene and abundant opaques. Photomicrograph taken with crossed polars.

Microscopically this basalt is holocrystalline with approximately 10 percent olivine (Fo_{86}) and clinopyroxene (augite) phenocrysts. The groundmass consists of microlitic plagioclase (An_{56}), clinopyroxene, olivine, and opaques. The microlitic plagioclase laths exhibit a moderately well developed pilotaxitic fabric. Groundmass plagioclase laths form an intergranular texture with clinopyroxene and olivine. Opaque crystals are commonly subophitic with olivine. Phenocrysts of olivine may show embayment along open fractures by groundmass.

BASALTIC FLOWS (undifferentiated) (Tbf)

Field Description

Macroscopically this basalt varies from light gray to black on weathered surfaces. Frequently there exists a buff colored weathering rind with a thickness of 3 mm. Phenocrysts of a visible size are not present. This dense and resistant basalt forms linear high standing dikes with associated minor flows. It may exhibit a slight flow layering which produces a slight platey regolith character.

Petrographic Texture

Basalt of this group is holocrystalline with 5 to 20 percent phenocrysts of plagioclase (An_{50}), clinopyroxene (augite ?), and minor olivine. The groundmass consists of plagioclase, clinopyroxene, olivine, and opaques which typically form a well developed pilotaxitic fabric (figure

7). Calcite is present as anhedral growths within vesicles. An intergranular texture is exhibited between groundmass crystals of plagioclase, clinopyroxene, and olivine. Opaque crystals occasionally occur in ophitic association with corroded plagioclase phenocrysts.

BISHOP PLACE BASALT (Tbpb)

Field Description

This basalt is brick-red and contains numerous small gas vesicles less than 1 mm in diameter. The color is due to a high degree of alteration producing iron staining. Visible unaltered basaltic stringers approximately 2 mm wide and 10 mm in length are common. This unit forms a low profile flow which exhibits a clinker-like texture. It erodes rapidly and contains large weathered vugs. Petrographic data is not available for this unit.

RHYOLITES OF THE ROUND MOUNTAIN VOLCANIC FIELD

General Statement

The rhyolites of the Round Mountain volcanic field have been classified in this study on the basis of color, texture, flow units, and geochemistry. These rhyolites are designated by map unit names that are informal and were given by the author. In all there are 10 rhyolite units which exhibit many similar macroscopic and microscopic textures. Because of this, a general field description is provided which is applicable to all of the rhyolites. Specific reference to distinctive features for the different flows is noted. A brief petrographic description of each unit is given in following sections. A more detailed description of the mineral optics and crystal habits is provided in Appendix C. Modal analytic results of 30 rhyolite thin sections is given in Appendix B.

Field Description

These rhyolites exhibit a wide variety of colors including buff, gray, black, lavender, purple, as well as combinations of these. A majority of the rhyolite units show many colors depending on the location of the outcrop. Texturally these rhyolites vary widely, not only between units, but also within a single unit.

Flow banding and other related flow structures are common throughout most of the rhyolites. Flow banding

(figure 8) is generally accented by variegated coloring of individual flow layers. Flow structures predominate in the Vivian rhyolite (Tvr), Andrus rhyolite (Tar), Gray rhyolite (Tgr), Perlite (Tpl), and Massive purple rhyolite (Tmpr). The intricate flow structures within these units enhance differential weathering along flow lines to produce a platey regolith on most slopes.

Brecciation textures (figure 9) are present chiefly in the Pumiceous flow rhyolite (Tpfr), Rhyolite breccia (Trb), and Lavender gray rhyolite (Tlgr) units. Such brecciation textures differ in color, clast size, clast shape, clast composition, and matrix. The breccia units exhibit spheroidal or bulbous-shaped outcrops due to preferential weathering of the interclast matrix material (figure 10). The clasts are predominately angular to subangular and range in size from approximately 1.4 m to 1 cm. The clast size generally decreases with increasing distance from the source vent. The clasts are composed of rhyolitic glass and commonly exhibit flow banded textures. The Pumiceous flow rhyolite may be classified as an autobrecciated flow rhyolite (Parsons, 1969) or as a pumiceous flow tuff. Numerous highly devitrified pumice clasts are present. Noticeable inclusions of basalt are incorporated in this unit and the olivine present in the basalt commonly exhibits a high degree of alteration.

The Perlite unit (Tpl) is chemically rhyolitic and contains numerous lenses of pure black obsidian set in a

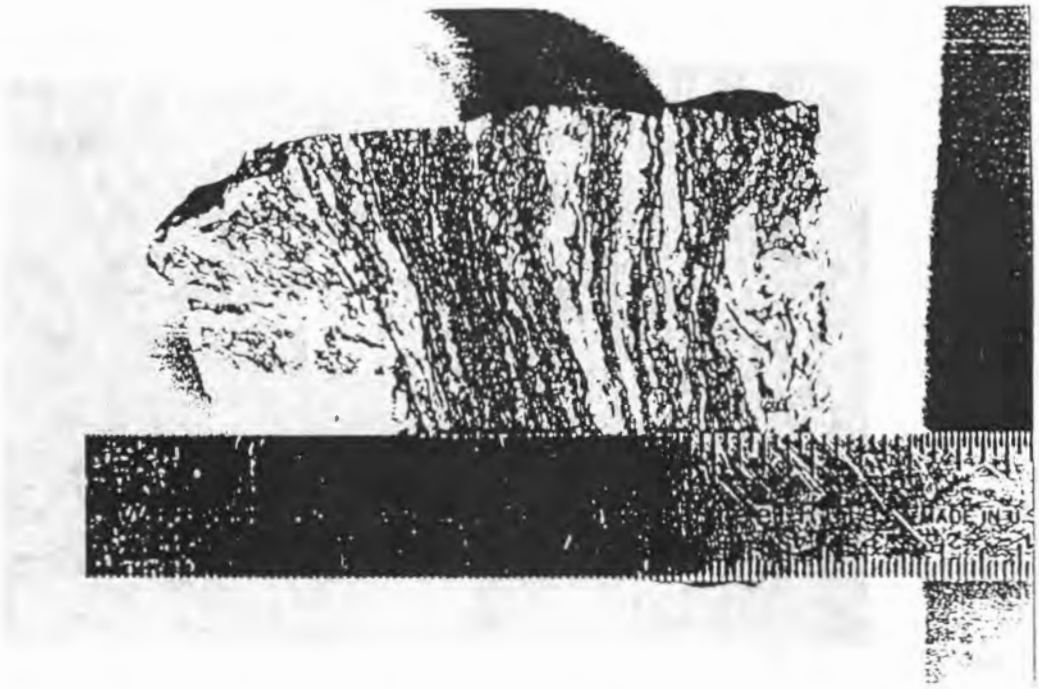

Figure 8 - Hand specimen of Vivian rhyolite exhibiting extensive flow banding and variegated coloring. Note the flow contortion feature at the right end of the sample.

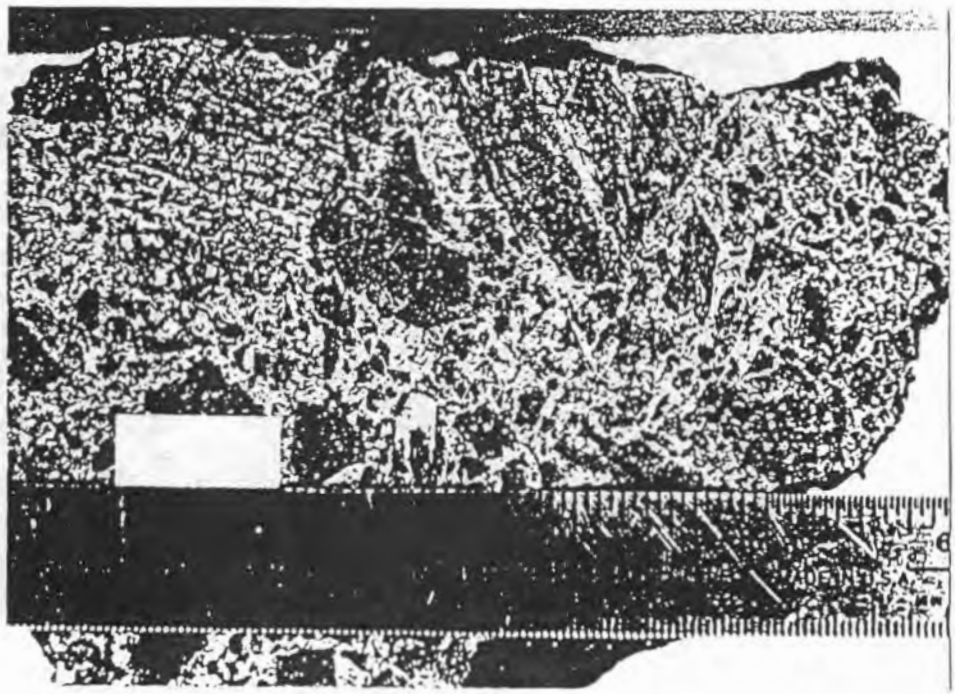

Figure 9 - Hand specimen showing the brecciation texture of the Rhyolite breccia (Trb) unit. Note the flow banded and obsidian breccia clasts contained within the highly devitrified matrix.

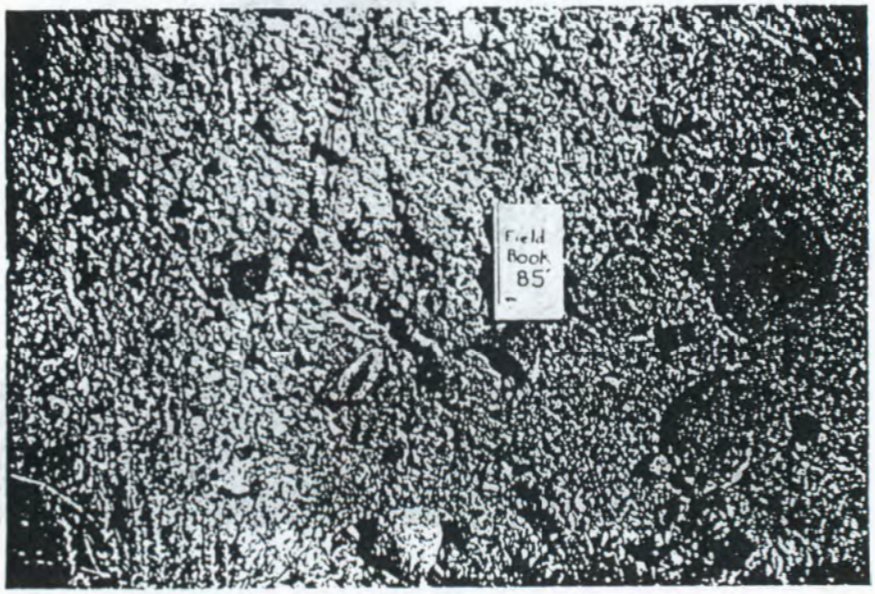

Figure 10 - Rhyolite breccia unit (Trb) exhibiting extensive weathering of the matrix surrounding breccia clasts.

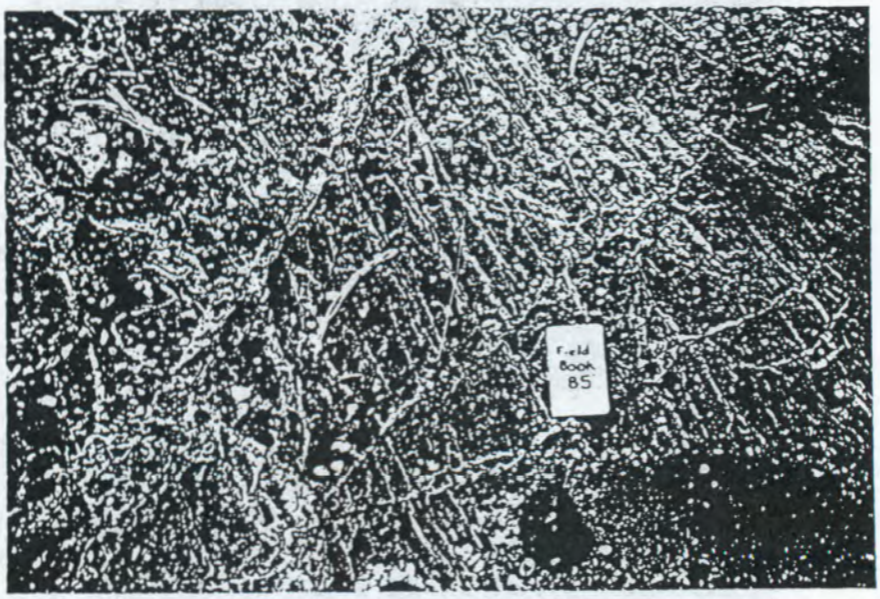

Figure 11 - Elongate lenses of obsidian in perlite unit (Tpl).

gray glassy matrix (figure 11). These lenses have an approximate elongation of 25:1 due to vertical compression or horizontal flow. This unit weathers rapidly to produce an obsidian regolith pavement.

The most prominent cliff forming unit is the Massive gray rhyolite (Tmgr). This rhyolite is very dense, highly resistant, and locally quite glassy. It exhibits a polygonal character due to the straight smooth fractures caused by frost wedging along jointing.

Petrographic Textures

Lavender Gray Rhyolite (Tlgr)

This is a relatively hypocrystalline rhyolite with 17 percent phenocrysts of sanidine, plagioclase (An_{24} - high oligoclase), quartz, biotite, and opaques set in a glass matrix. The resulting texture is vitrophyric. Perlitic fracturing (figure 12) is common along with microfractures that follow phenocryst boundaries. Sanidine may be embayed by plagioclase or contain ophitic plagioclase microlites. Minor exsolution of sanidine is present but rare.

Vivian Rhyolite (Tvr)

A virtually holohyaline rhyolite containing cryptocrystalline sanidine, quartz, plagioclase, opaques, and minor clinopyroxene. Flow banding is prominent with minute feldspar crystals producing a hyalopilitic texture. Spherulites, both single and compound, composed of radiating

Figure 12 - Photomicrograph (35x) of extensive perlitic fracturing in a sample of Lavender Gray rhyolite (Tlgr). Photomicrograph taken under plane polarized light.

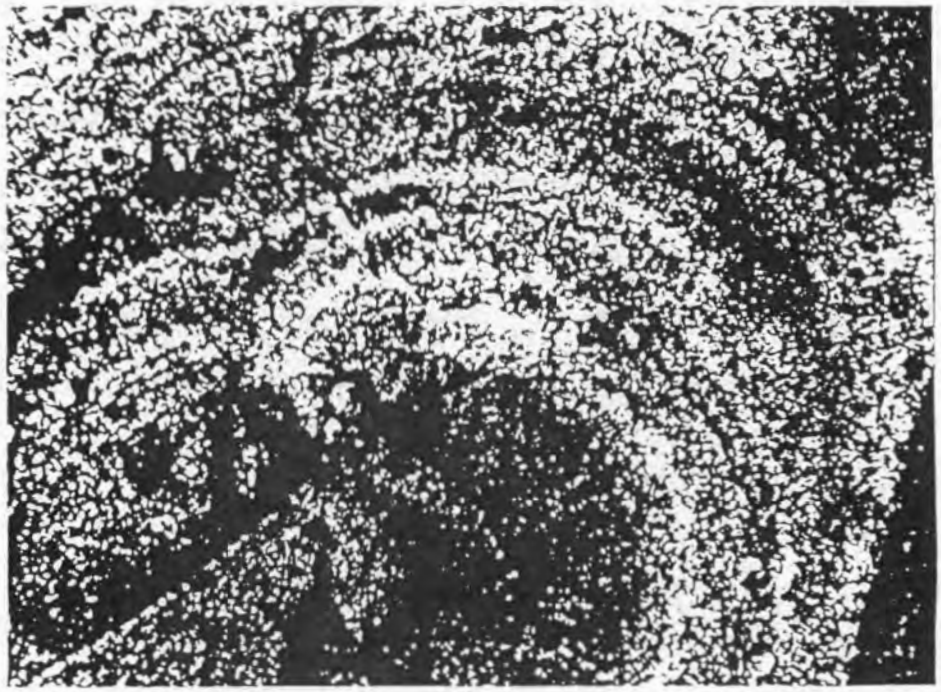

Figure 13 - Photomicrograph (35x) of a spherulite composed of radiating feldspar and quartz crystallites. The photomicrograph of this sample of Massive Purple rhyolite was taken with crossed polars.

feldspar (sanidine ?) and quartz crystals are numerous. Perlitic fracturing of the matrix is minor.

Andrus Rhyolite (Tar)

This rhyolite is hypocrystalline with 3 to 20 percent phenocrysts of sanidine, plagioclase (An_{24}), and minor quartz, biotite, opaques, and clinopyroxene. Gas vesicles commonly contain secondary quartz crystallization. A pilotaxitic sanidine microlite texture is frequently present. Glomeroporphyritic clots of plagioclase, sanidine, and quartz are present. Embayment of sanidine phenocrysts by matrix is rare.

Buff Rhyolite (Tbr)

This unit is a hypocrystalline rhyolite containing 8 to 15 percent phenocrysts of plagioclase (An_{24}), sanidine, and quartz set in a glass matrix. Perlitic fracturing is common along with a well-developed flow banding of the matrix. Glomeroporphyritic clots of plagioclase and sanidine phenocrysts exhibit a subophitic relationship. Gas vesicles are occasionally numerous and elongate in form.

Massive Gray Rhyolite (Tmgr)

This unit is essentially equivalent to the Buff rhyolite in mineral habit and fabric. Flow banding is not well-developed. The occurrence of perlitic fracturing and gas vesicles is rare. The matrix is composed of 30 percent

glass and 70 percent cryptocrystalline feldspar (sanidine ?) and quartz. Quartz occasionally forms stringers and discrete glomeroporphyritic pods.

Gray Rhyolite (Tgr)

This hypocrystalline rhyolite is quite similar in texture and mineralogy to the Massive gray rhyolite. Exceptions which distinguish these units include fewer phenocrysts in the Gray rhyolite which are surrounded by cryptocrystalline feldspar and quartz. Flow banding of the matrix may or may not be present. Elongate gas vesicles commonly contain internally radiating growths of fiberous feldspar (?) and quartz. Glomeroporphyritic clots of plagioclase and sanidine are present with minor biotite and quartz.

Perlite (Tpl)

This description is applicable only to the obsidian lenses within the Perlite unit. These lenses are holohyaline with minor flow banding and vein structures containing cryptocrystalline feldspar, quartz, and opaques. Micro-spherulites (<.1 mm) of quartz and feldspar are common. Pyroxene (?) trichites radiating from opaque cores are abundant.

Massive Purple Rhyolite (Tmpr)

This unit is a predominantely holohyaline rhyolite with

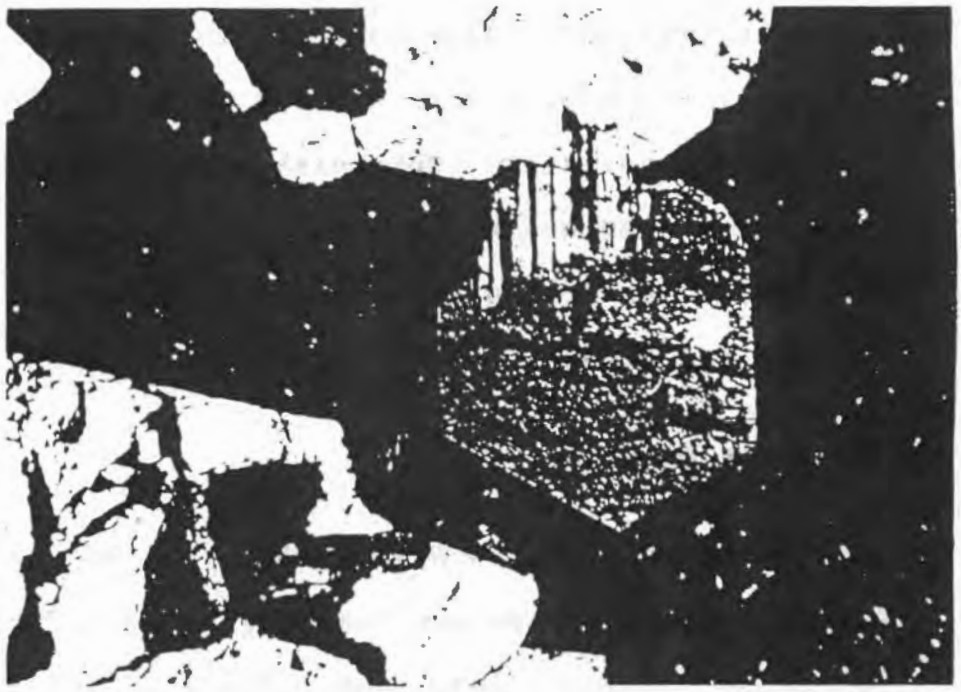

Figure 14 - Photomicrograph (35x) of the detachment of a euhedral phenocryst of sanidine from a larger sanidine crystal set in a glass matrix (black). Note the subophitic relationship of the sanidine and plagioclase phenocrysts. This photomicrograph of Rhyolite breccia (Trb) was taken with crossed polars.

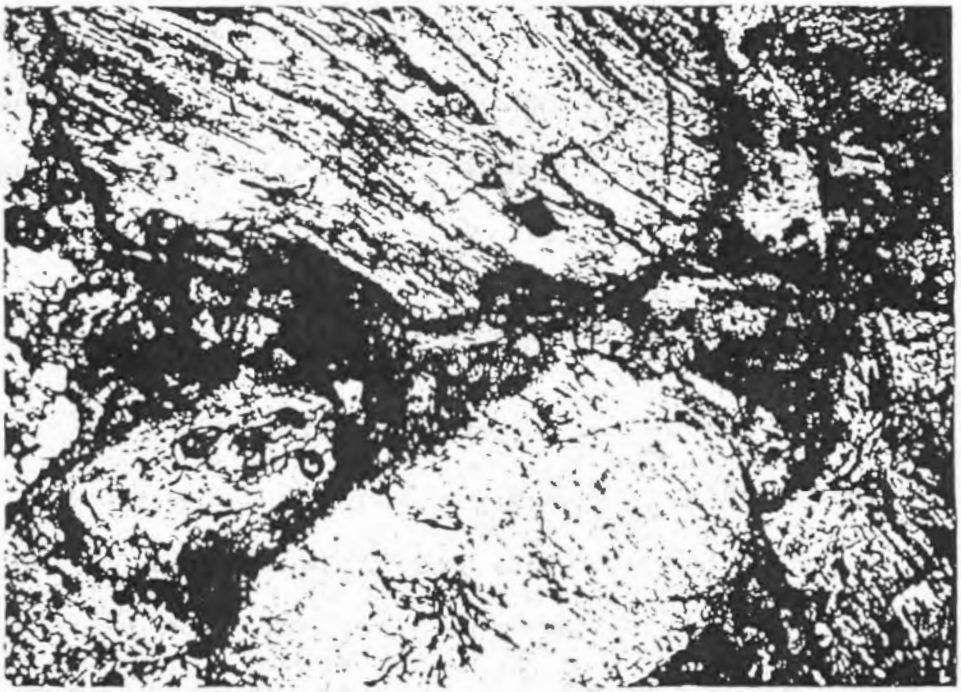

Figure 15 - Photomicrograph (35x) of Rhyolite breccia (Trb) unit exhibiting small scale brecciation textures. The clasts have flow banding and are completely holohyaline. This photomicrograph was taken under plane polarized light.

minor cryptocrystalline feldspar and quartz. Flow banding is well developed with sinuous layering of feldspar and quartz crystallites. Spherulites (figure 13) consisting of radiating needle-like crystals of feldspar and quartz are numerous. Branching structures composed of feldspar and quartz are common.

Rhyolite Breccia (Trb)

This rhyolite is hypocrystalline to holohyaline with approximately 15 percent phenocrysts of plagioclase (An_{24}), sanidine (figure 14), and minor quartz, biotite, and opaques. Brecciation textures (figure 15) predominate with angular clasts of glass surrounded by a perlitic fractured flow glass. The rhyolite contains occasional inclusions of highly altered olivine basalt. Overall granularity may appear hypidiomorphic due to the fragmentation of phenocrysts. Pyroxene (?) trichites are common in the glass matrix.

Pumiceous Flow Rhyolite (Tpfr)

This is a hypocrystalline rhyolite with 5 percent phenocrysts of anhedral plagioclase, sanidine, and quartz. It contains numerous basalt inclusions of various textures and mineral assemblages. Brecciation textures predominate and minor layering of glass shards produce flow tuff characteristics. Clasts of pumice and flow banded glass are numerous.

PETROLOGY OF THE ROUND MOUNTAIN VOLCANICS

General Statement

Chemical analyses using whole rock x-ray fluorescence methods were performed on 17 rhyolite samples from the study area. Of these 17 samples, only the Lavender Gray rhyolite and the Gray rhyolite units were not chemically analyzed. Chemical analyses of 7 basaltic specimens were also completed. All chemical analyses were performed by the X-ray Assay Laboratories Inc., Don Mills, Ontario, Canada. The analyzed units include the Williams basalt, Josep basalt, Field Dam basalt, and Basalt Flows (undifferentiated). The Vernon and Bishop Place basalts were not chemically analyzed. The chemical analyses yielded both major and trace element data. The trace elements included in the analyses are Cr, Rb, Sr, Y, Zr, Nb, and Ba. Results of the major chemical analyses and CIPW normative calculations are provided in Appendix D. Trace element results are given in Appendix E.

Rhyolites

All the rhyolites analyzed have virtually identical major chemical contents, with the exception of the Pumiceous Flow rhyolite (Tpfr) or tuff. It should be noted that the sample of Pumiceous Flow rhyolite (27-1) exhibits a similar but distinct chemical expression due to its high percentage

of volatiles (11.7 LOI) and numerous basaltic inclusions. These basaltic inclusions lower the total SiO_2 content and produce slight increases in Al_2O_3, FeO, MgO, and CaO percentages. This sample plots uniquely on all chemical diagrams (figures 16, 19, 20, 21).

Major element chemical data were plotted on Harker variation diagrams (figure 16) to express the homogeneity of these rhyolites. The weight percentage of SiO_2 varies from 72.8 to 76.6 (LOI uncorrected) and 76.06 to 76.75 for normalized results. Soda (Na_2O) and K_2O range from 4.01 to 4.60 percent (LOI uncorrected), and 4.45 to 4.87 percent (normalized). Alumina (Al_2O_3) content for the rhyolites is also tightly grouped and ranges from 13.01 to 13.40 percent (normalized).

These rocks have been classified as rhyolites (figure 17) based on normative color index (Ol+Opx+Cpx+Mt+Il+Hm) versus normative plagioclase composition (100 An/(An+Ab+5/3Ne)) plots (Irvine and Baragar, 1971). Chemical classification (figure 17) of these rhyolites based on K_2O and SiO_2 abundances, groups them all as high-K rhyolites (Barker, 1981). Plots of total alkalies (Na_2O + K_2O) and SiO_2 place these rhyolites in the subalkaline field.

Trace element variation diagrams (figure 20) for these rhyolites show them to be very similar in Cr, Sr, Ba, and Zr abundances. Based on the abundances of Rb, Y, and Nb the rhyolite units have distinctive expressions. These rhyolites exhibit variation in Rb, Y, and Nb amounts ranging

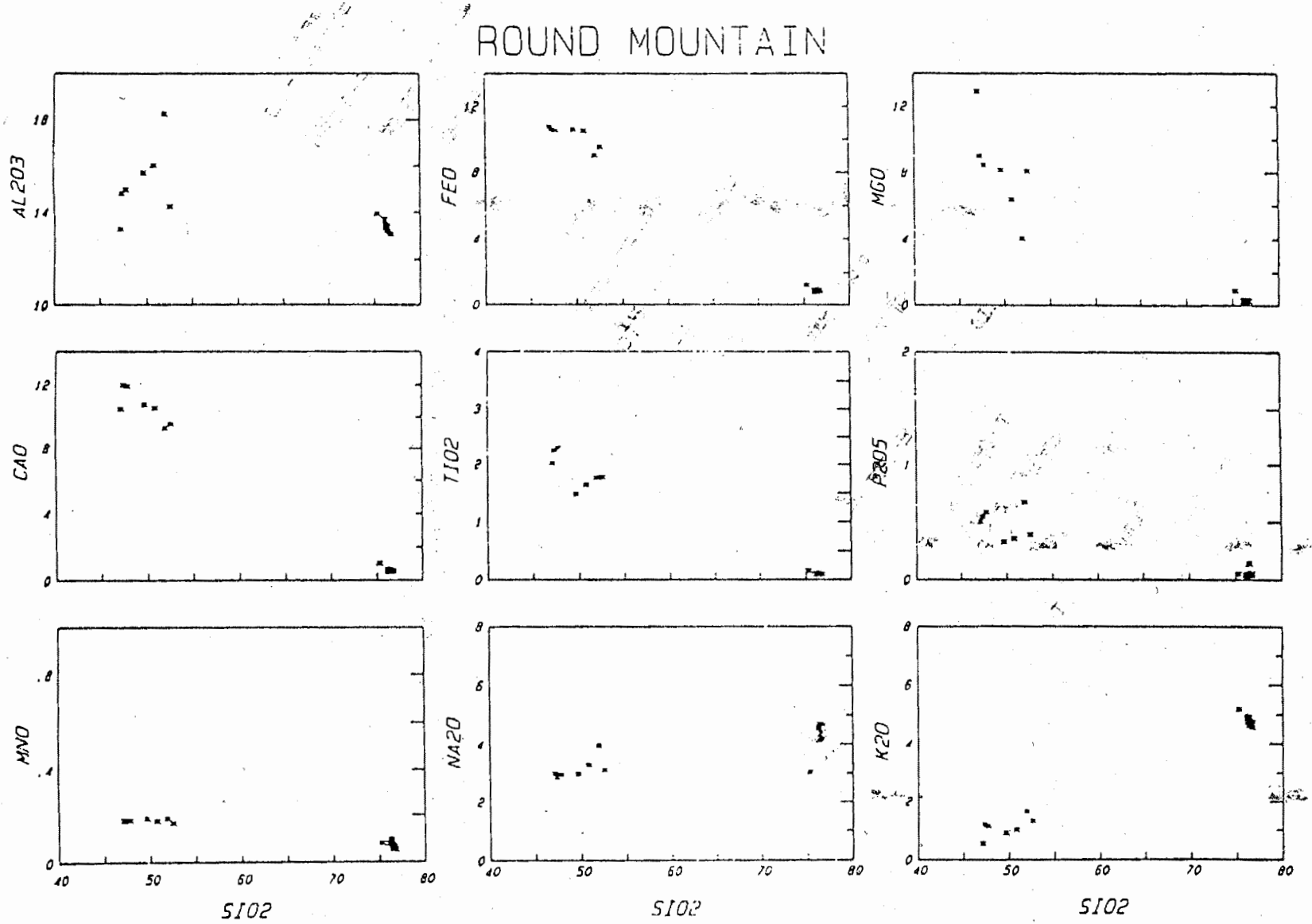

Figure 16 - Major chemical variation diagrams showing weight percent of Al_2O_3, FeO, MgO, CaO, Na_2O, K_2O, P_2O_5, TiO_2, and MnO plotted against SiO_2. Basalts and rhyolites of the Round Mountain volcanic field are plotted.

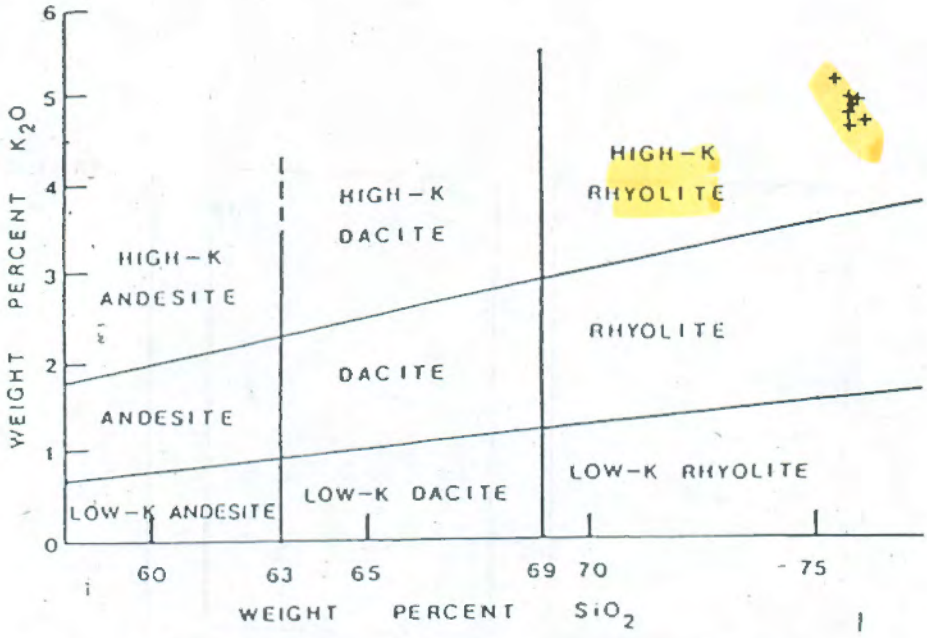

Figure **17** - Chemical classification of andesite, dacite, and rhyolite based on weight percent K_2O and SiO_2. The Round Mountain rhyolites (+) plot as high-K rhyolites. (After Barker, 1981)

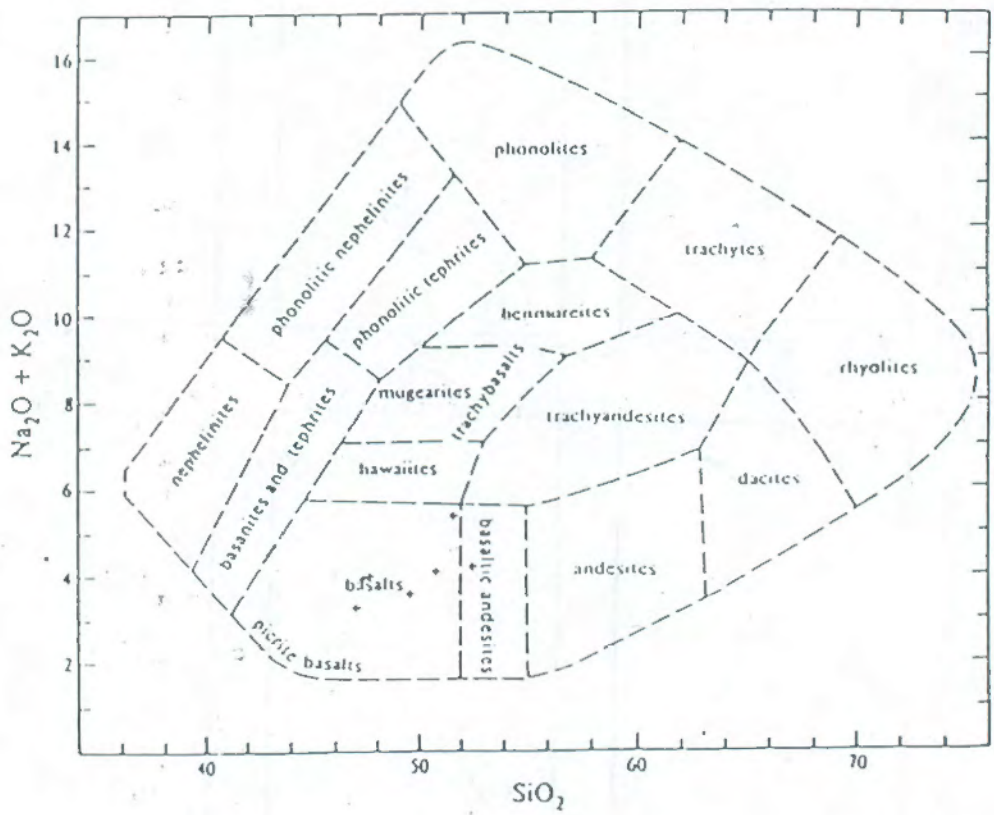

Figure **18** - Classification of non-potassic volcanic rocks based on total alkalies and SiO_2. The alkali olivine basalts (+) of Round Mountain plot as basalts and borderline basaltic andesites. (After Cox et al., 1984)

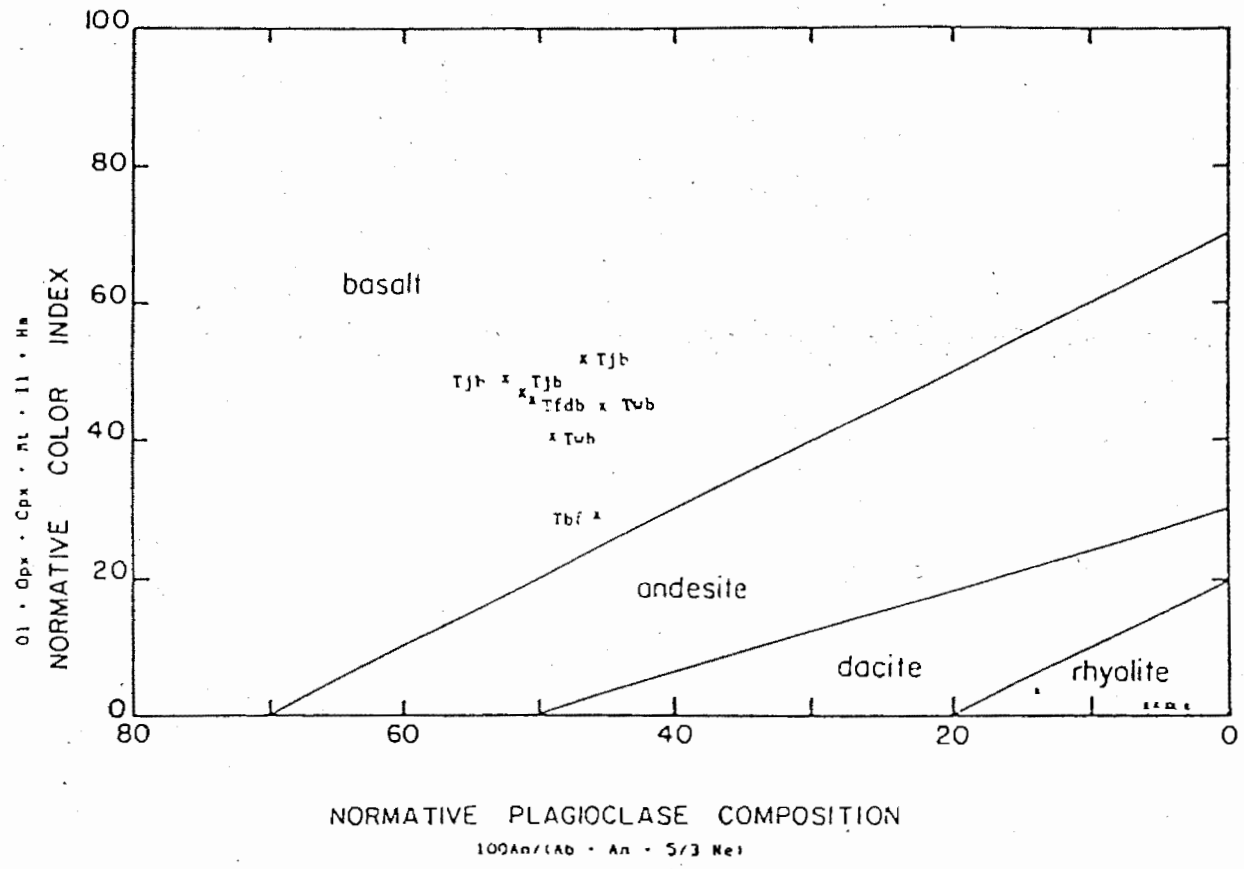

Figure **19** - Classification of the alkali olivine basalts (unit labeled X) and rhyolites (X) of the Round Mountain volcanic field based on normative color index and normative plagioclase composition (Williams basalt - Tub, Josep basalt - Tjb, Field Dam basalt - Tfdb, Basalt flows - Tbf). Plots are in cation equivalents. (After Irvine and Baragar, 1971)

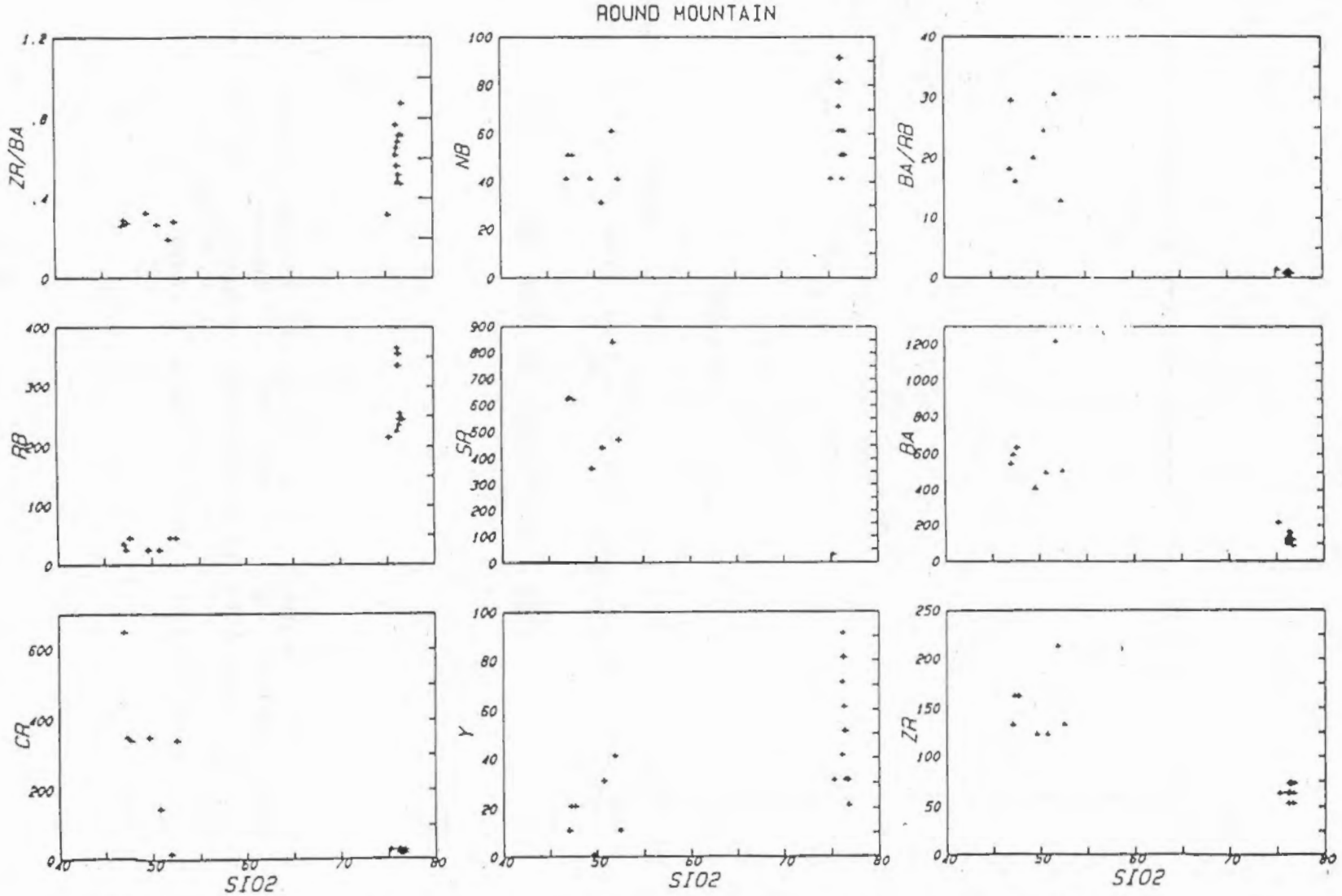

Figure 20 - Trace element variation diagrams showing Cr, Rb, Sr, Y, Zr, Nb, Ba, Zr/Ba, and Ba/Rb abundance (ppm) plotted against weight percent SiO_2. Basalts and rhyolites of the Round Mountain volcanic field are plotted.

from 210 to 360 ppm, 20 to 90 ppm, and 40 to 90 ppm respectively. A noticeable gap in the distribution of Rb occurs between 250 to 330 ppm. This hiatus in data provides a clear distinction between the rhyolties sampled in the southern portion of the study area to those of Round Mountain itself. The southernmost rhyolites sampled have Rb values of 210 to 230 ppm while those of Round Mountain are 330 to 360 ppm. This separation of trace element abundances with respect to sample location occurs also for Y and Nb without a visible break in the distribution of data. The southern rhyolites have values of 20 to 50 ppm and 40 to 60 ppm for Y and Nb respectively. The rhyolites of Round Mountain have Y and Nb abundances of 50 to 90 ppm and 70 to 90 ppm respectively.

The trace element analyses have provided data to indicate that the geologic map (plate 1) prepared for the study area may have minor discrepancies. The geologic map was prepared on the basis of field identification and expression of the volcanic units, along with major chemical and petrographic information. Trace element analyses of the rhyolite units indicate that the mapped exposure of the Andrus rhyolite (Tar) and Rhyolite breccia (Trb), to the south of Round Mountain, may not be contiguous with the exposures of these units on Round Mountain. The Andrus rhyolite mapped to the south of Round Mountain is equivalent, with respect to trace element abundances, to the Vivian rhyolite (Tvr) unit. Conversely, the Rhyolite

breccia unit in the southern study area is not equivalent, with respect to trace element abundances, to the breccia unit mapped on Round Mountain.

Basalts

The basaltic rocks in and around the Round Mountain volcanic field exhibit a fair amount of variation in both major and trace element abundances. It should be noted that one sample, (# 29-6 Basalt Flows - undifferentiated), has anomalous trace element and some major element values relative to the rest of the basaltic suite of the area. This sample is virtually out of the study area however and exhibits no relationship to any of the Round Mountain volcanic events.

The rocks have been classified (figure 18) as basalts and borderline basaltic andesites based on total alkalies and SiO_2 abundances (Cox et al., 1984). These rocks plot in the basaltic field based on Irvine and Baragar's (1971) classification system using normative color index and normative plagioclase composition (figure 19). More specifically, specimens (4-8, Tfdb), (27-2, Twb), and (28-2,28-3, Tjb) are basalt with specimen (27-4, Twb) being a basaltic andesite. The classification of sample (27-4) as a basaltic andesite is believed to be caused by the occurrence of quartz xenocrysts modifying the results of the chemical analyses. The inclusion of these xenocrysts may

have increased the SiO_2 content sufficiently to place the specimen in the basaltic andesite field.

The SiO_2 content in these basalts ranges from 47.02 to 52.49 percent (normalized). Excluding specimen (29-6, Tbf), the total alkali content for these basalts range from 3.37 to 4.26 percent (normalized). Based on MacDonald's (1968) classification (figure 21a) of alkaline and tholeiitic suites using $Na_2O + K_2O$ versus SiO_2 plots, these basalts are alkaline with the exception of specimen (27-4, Twb) lying in the tholeiitic or subalkaline field. Classification of the basalts using Irvine and Baragar's (1971) redefined alkaline-subalkaline discrimination boundary, designates only the samples (28-2, 28-3, 28-5) of the Josep basalt as alkaline, excluding (29-6, Tbf). Based on AFM plots (figure 22) comparing the patterns of variation of tholeiitic, alkaline, and calc-alkaline suites (Irvine and Baragar, 1971), the basalts of Round Mountain are interpreted as having an alkaline trend. This classification is subjective however due to the insufficiency of available data. There is a slight iron enrichment trend, but this may be consistent with rocks of tholeiitic or alkaline suites.

The argument for an alkaline character of the Josep basalt samples (28-2, 28-3, 28-5) may be supported by the Yoder and Tilley (1962) Di-Fo-Ne-Qz tetrahedral classification system. The Josep basalt specimens lie in the alkali olivine-basalt field on the Ne side of the "critical plane of silica undersaturation", while the

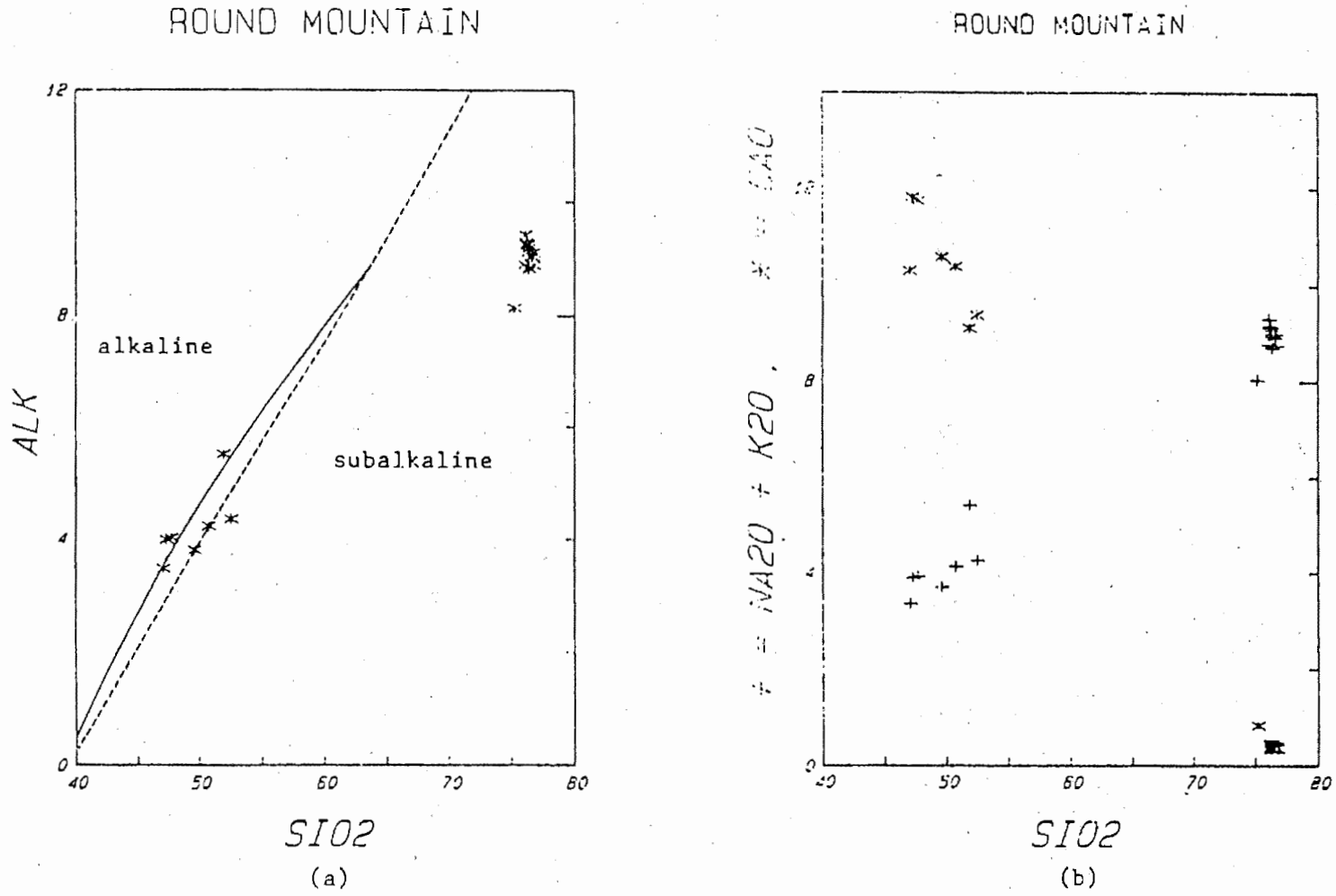

Figure **21** - Plot of alkalies versus silica (a) and alkalies and CaO versus SiO_2 (b) for the alkali olivine basalts and rhyolites of the Round Mountain volcanic field. Dashed line is MacDonald's (1968) dividing line for alkaline and tholeiitic rocks. Solid line is Irvine and Baragar's (1971) adjusted alkaline-tholeiite boundary.

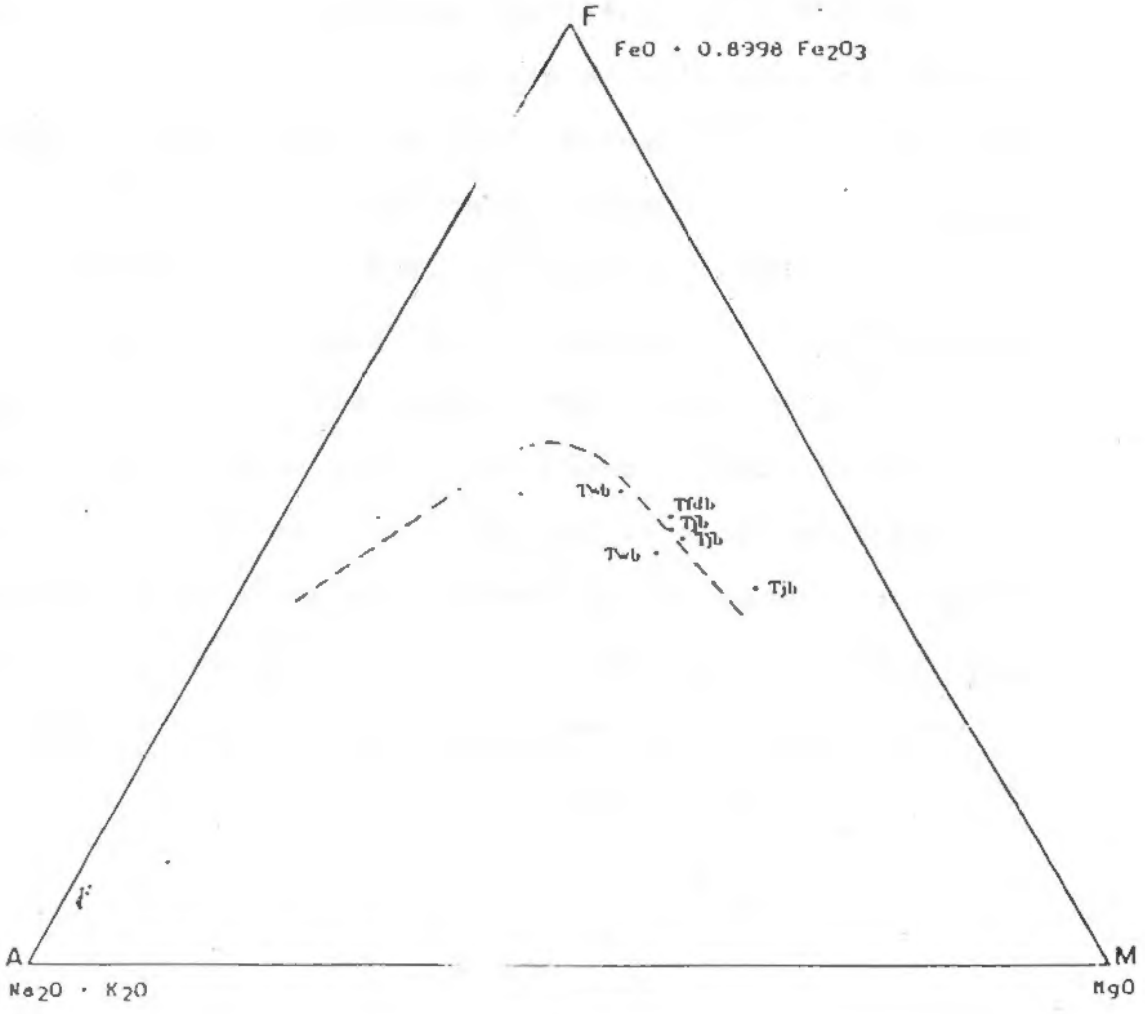

Figure 22 - AFM diagram c aring the compositional trend of alkali olivine basalts (unit labeled and rhyolites (+) of the Round Mountain volcanic field (Williams basalt wb, Josep basalt - Tjb, Field Dam basalt - Tfdb, Basalt flows - Tbf). The shed line separates the tholeiitic (above) and calc-alkaline compositions ter alkaline compositions were removed. (After Irvine and Baragar, 1971)

remaining basalts lie in the olivine tholeiite field. The presence of normative Ne in the three Josep basalt samples, averaging 2.7 percent, places them into the alkali olivine-basalt field by necessity. Nepheline is not present in thin sections of these basalts.

Trace element variation diagrams (figure 20) show these basalts to generally be grouped with other samples of the same unit. More specifically the Josep basalt samples form a fairly tight grouping, as do the Williams basalt samples for most trace elements, with the exception of Cr abundances. It is worth noting that the specimen (29-6, Tbf) exhibits high Sr, Ba, and Zr values of 830 ppm, 1200 ppm, and 210 ppm respectively. This specimen also has low Cr abundances of only 10 ppm. This enrichment in Sr and Ba along with low Cr abundances may be consistent with a few percent (<5) of fractional melting of a lherzolitic (clinopyroxene, orthopyroxene, olivine, and spinel) mantle composition (Gast, 1968).

EMPLACEMENT AND ERUPTIVE HISTORY OF ROUND MOUNTAIN

General Statement

The Round Mountain volcanic field consists of various rhyolite domes and flow units along with basaltic domes, flows, dikes, and cinder cones (figure 23). These constructs are the products of a complex volcanic history. Based on field observations, petrographic examinations, and geochemical data, a developmental model of the volcanic complex has been constructed.

The major rhyolitic dome of the volcanic field is Round Mountain. Field evidence suggests that Round Mountain underwent both endogenous and exogenous phases in its development. Initial periods of development were mainly endogenous and were followed by successive exogenous stages which modified the dome's physiographic expression. Observation of the stratigraphy of the volcanic units associated with the dome reveal information on which to base a relative measure of the amounts of volcanic material erupted during each phase. The endogenous phase expressed in the field represents approximately 30 to 40 percent of the total rhyolite erupted, with the remaining 60 to 70 percent of the rhyolitic volcanics being of exogenous nature.

The major phases of emplacement of the Round Mountain volcanic complex have been grouped into six stages. These

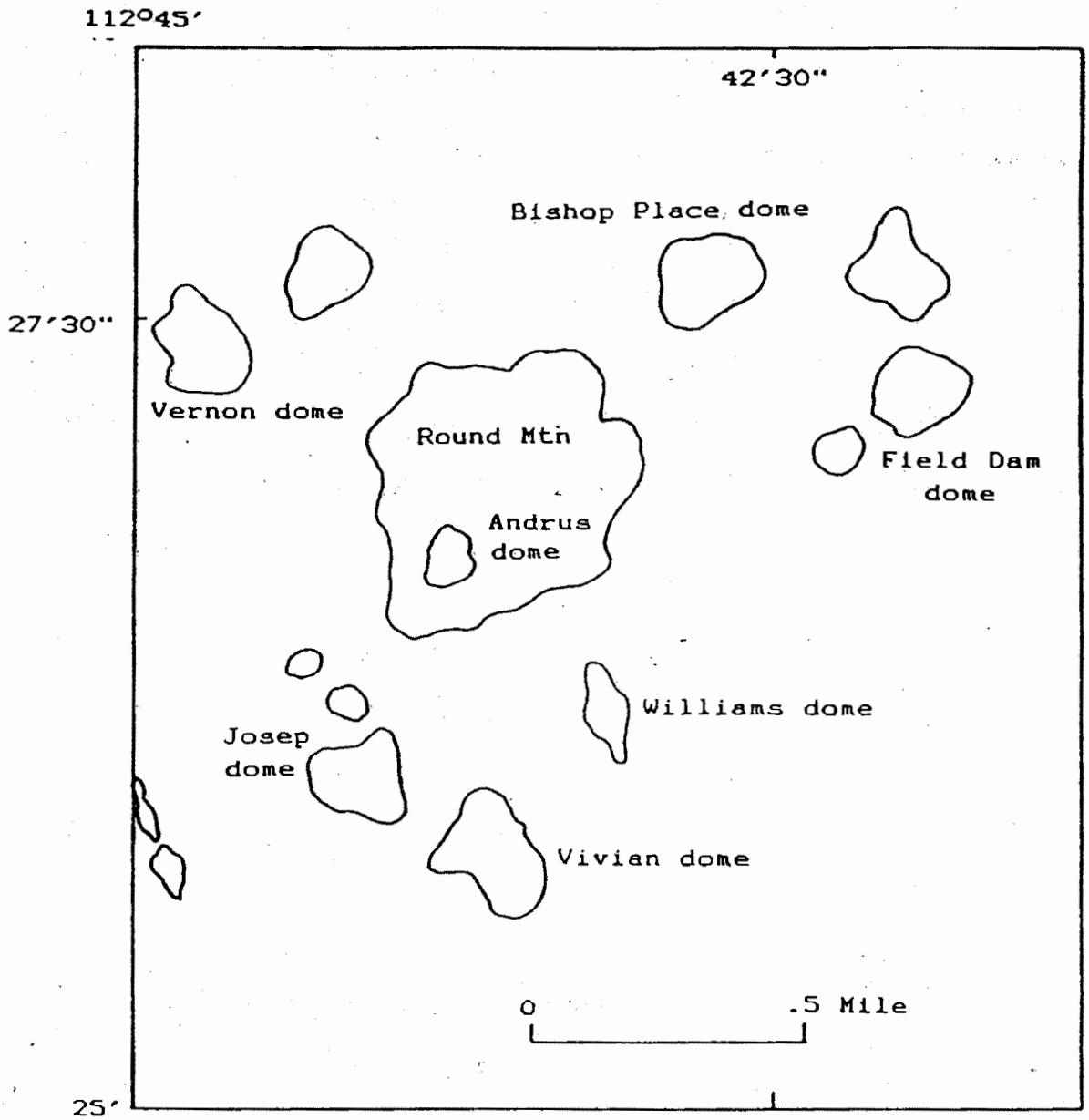

Figure 23 - Generalized map of the Round Mountain area showing the locations of the volcanic constructs. The construct names are informal and given by the author.

stages represent the sequence of volcanic development, some of which may have been synchronously evolving events.

Stage 1

Initiation of volcanic activity requires the generation of a driving heat source. This stage involved the emplacement of a basaltic magma, acting as the heat source, into the upper crust (figure 24). The basaltic intrusion used in this model is derived by partial melting of the mantle. Best and Brimhall (1974) suggest that source regions for the late Cenozoic alkali basalts of the Grand Canyon region are from depths of 65 to 95 km. This estimate is based on the generation of alkali olivine basalt magmas by incremental partial melting of a peridotite mantle at 20 to 30 kb. The upper crust, having a granitic composition, is believed to be the most likely site of emplacement for the subsequent formation of a rhyolitic magma.

Crustal structure in the Round Mountain region was a dominant control affecting the location of the initial basaltic emplacement. The two major phases of structural adjustment in northern Arizona were (1) from latest Cretaceous to late Eocene, and (2) from Miocene to present (Shoemaker et al., 1974). The later phase of adjustment involved large displacement normal faulting and thus led to the development of major structural blocks (figure 1, 2)

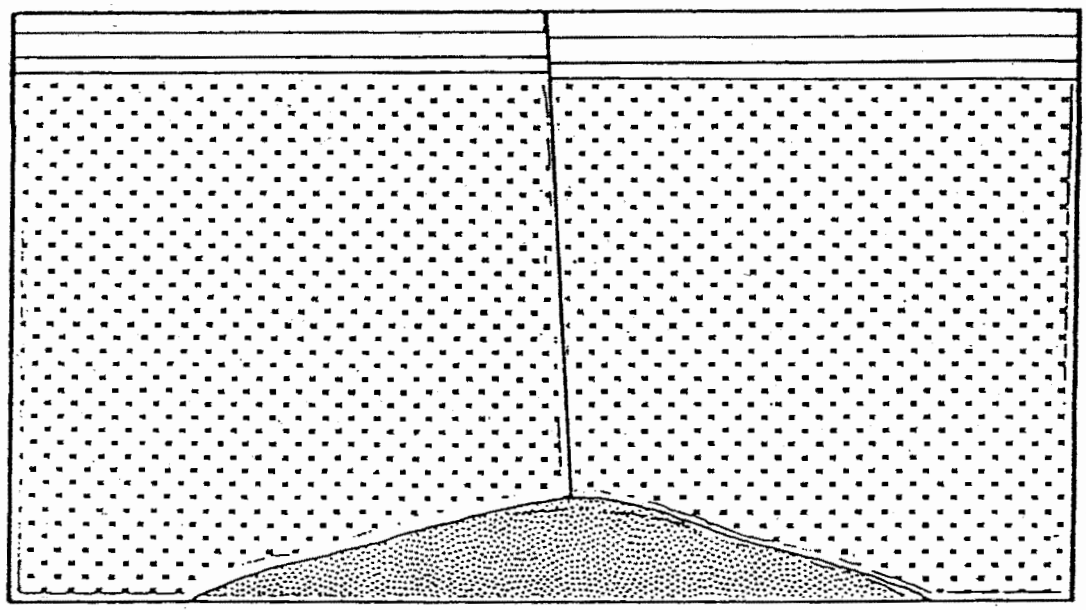

Figure 24 - (STAGE 1) Emplacement of basaltic magma into the upper crust along zone of weakness (fault or fracture system).

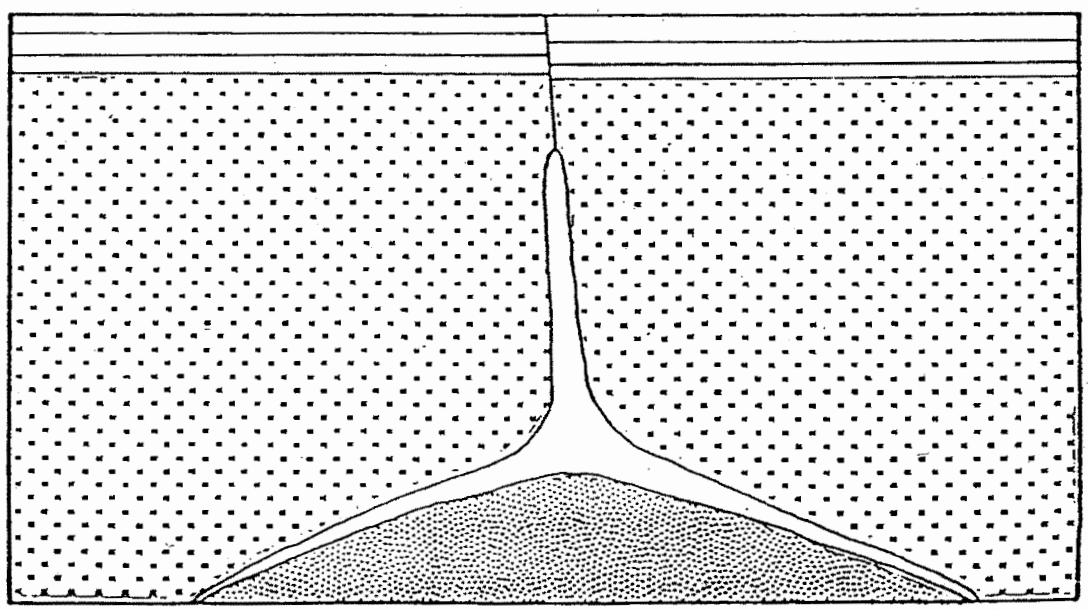

Figure 25 - (STAGE 2) Rhyolite formation by partial melting of the crust caused by the basaltic intrusion. Rhyolitic magma migrates preferentially along fracture zone.

delineated by the fault systems. These fault systems are presumed to extend to considerable depths in the crust and are thus largely responsible for controlling the sites of basaltic emplacement on a regional scale. The sites of volcanic centers in northern and central Arizona (figure 1) form lineaments parallel to these fault systems and are believed to be controlled by them (Eastwood, 1974; Shoemaker et al., 1974).

Stage 2

An upper crust of granitic composition is suggested as the most likely site of emplacement for the subsequent formation of a rhyolitic magma (figure 25). Eichelberger and Gooley (1977) suggested that since deep regions of the crust have high temperatures, it follows that they are most likely to yield substantial amounts of rhyolitic magma due to the emplacement of a hot basaltic intrusion. However problems arise with causing small amounts of rhyolitic magma to migrate to the surface without a basaltic heat source as a driving mechanism. Therefore due to the very small amount of rhyolite erupted in the Round Mountain volcanic field, the upper crust was selected as the region for the generation of the rhyolitic magma.

The contact of the basaltic magma with the granitic host rock is believed to have caused partial melting at granite minimum temperatures to yield the rhyolitic magma.

Based on thermal calculations, partial melting of a granitic crust due to the emplacement of a basaltic intrusion, is an efficient process to generate rhyolitic magma (Lachenbruch et al., 1976).

After a sufficient amount of rhyolitic magma was generated, magmatic migration began preferentially along a fracture or fault zone. Fault zones provide an infinite permeability for a fluid medium relative to the surrounding country rock and thus would allow rapid upward migration of the newly generated rhyolitic magma.

The bimodal nature of the Round Mountain volcanic field is, in part, a consequence of fault or fracture zones being present. Christiansen and Lipman (1972) have shown that a change from intermediate to bimodal volcanism in the western United States correlates well with the time when block faulting began in the region. This reflects the importance that block faulting may have on controlling the petrologic character of volcanic events. More specifically, it indicates that block faulting may greatly reduce any mixing of basaltic and rhyolitic magmas by allowing a rapid upward migration of the rhyolitic magma. The short residence time of the magmas at depth allows for little modification by fractionation processes.

If mixing of basaltic and rhyolitic magmas occurred, it would result in the formation of hybrid magmas which would lie along a linear mixing line between the basaltic and

rhyolitic whole rock compositions (Eichelberger and Gooley, 1977). The degree of hybridization depends on the residence time of the two differing magmas, the geometry of the interface, and turbulance of the liquids (Yoder, 1973). Mechanical mixing coupled with the intimate contact of a basaltic liquid with a rhyolitic liquid, results in the formation of various petrographic textures such as crenulate margins of basic masses, and wisp-like basic inclusions contained within a silicic matrix (Blake et al., 1965). Neither the textures related to mixing, nor rocks of hybrid compositions are present in the Round Mountain volcanic complex. This adds further support to the hypothesis that fault or fracture zones controlled the location and rate of upward migration of the rhyolitic magma.

Stage 3

The upward migration of rhyolitic magma along a fault zone continued (figure 26) and ultimately the magma breached the surface. The initial eruptive event consisted of a pumiceous flow (tuff) unit. The total areal extent and thickness of this basal unit are not specifically known, due to the blanketing of this unit by latter eruptive events. Based on field observations, this pumiceous flow (tuff) unit has a maximum estimated thickness of 15 meters. This flow unit is observed only in the south sector of the Round Mountain volcanic complex. The unit extends a minimum of

2.4 km to the south of its presumed source vent. This biased southward flow direction implies eruption from an asymmetric vent, or an indication for a southward sloping topography of the surroundings at the time of eruption.

Chemically this pumiceous flow is rhyolite but it has been designated as a pumiceous flow rhyolite (tuff) based on its texture. This unit contains some glass shards indicative of pyroclastic activity. The highly devitrified matrix of this unit contains many subangular fragments of pumice, glass, and minor basalt. The basaltic inclusions are thought to have been accidentally incorporated into the flow as it spread laterally over the surrounding plain. The basaltic fragments, along with a few rounded inclusions of various lithologies, may have been Tertiary gravels lying on the surface at the time of eruption. Such gravels were deposited on the Coconino Plateau from sources to the south in early to middle Tertiary (Young, 1982).

This pumiceous flow rhyolite (tuff) is similar to an initial perforation breccia as described by Parsons (1969) based on the angular to subangular texture of inclusions. However this unit has been designated as a rhyolite flow (tuff) based on the presence of some flow features exhibited by the unit that are not present in perforation breccias.

The abundance of pumice fragments and the light density of the frothy glass matrix infers that the magma came in contact with water during eruption. The contact was most

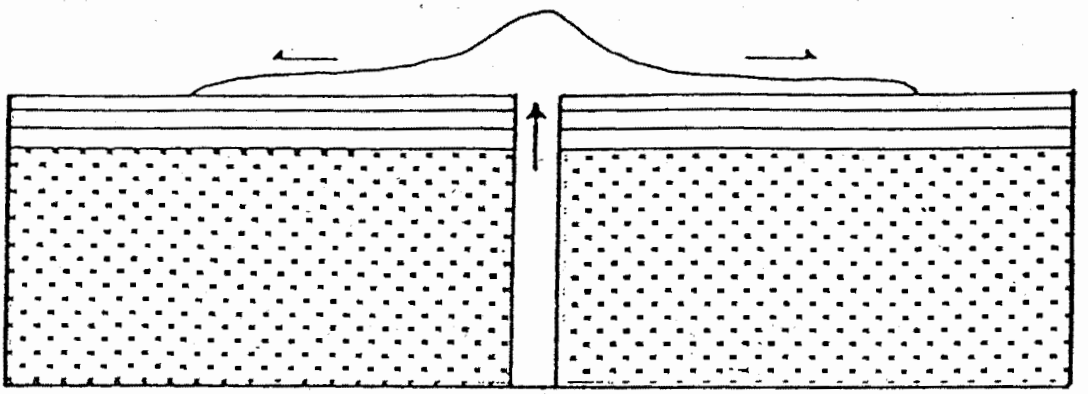

Figure 26 - (STAGE 3) Continued upward migration of rhyolitic magma breaching the surface. Initial flows are pumiceous due to the contact of magma with water laden sedimentary rocks.

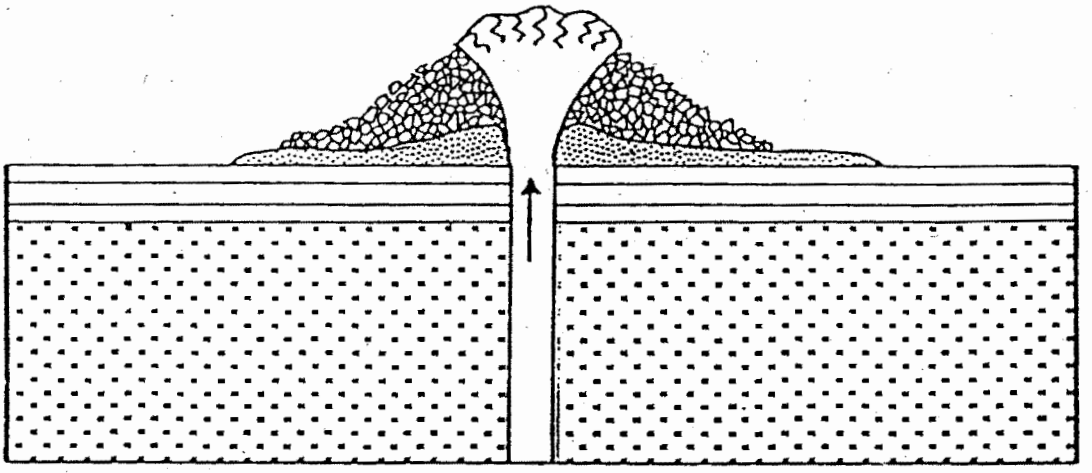

Figure 27 - (STAGE 4) Major growth exhibiting typical endogenous dome development, intimate contact between the extruding magma and the crumble breccia produce a massive unit.

likely made as the rhyolitic magma perforated the water charged sedimentary strata of the Plateau. This would lead to the formation of pumice, glass, and possibly some pyroclastic activity which would have contributed tephra (Parsons, 1969).

Stage 4

This stage of dome development involved both early and late eruptive phases. The existence of two separate but related phases is reflected by both trace element data and field observations.

Examination of the trace element abundance distributions of the rhyolites of the Round Mountain volcanic field reveal the presence of 2 separate but related phases of rhyolitic magma generation. More specifically, Rb, Nb, and Y abundances exhibit a separation (figure 20) between those rhyolite units of the southern study area from those of Round Mountain. Enrichment of Rb from 210 to 360 ppm and Nb from 40 to 90 ppm is not easily explained by fractionation processes within a single magma chamber. Since Rb and Nb follow potassium in crystal fractionation and sanidine is the major phenocryst phase present in these rhyolites, it is probable that a two magma chamber source may be responsible for these trace element abundance variations. Using this information, it is suggested that a vent to the south of Round Mountain was the source for the

rhyolite units exposed in the southern portion of the study area. Likewise the rhyolites of the Round Mountain dome were erupted from a separate vent and magma chamber.

The rhyolite units of the southern portion of the study area erupted prior to those of Round Mountain. Evidence for this relative age relationship is expressed by the rhyolite units immediately to the south of Round Mountain. These units dip south approximately 15°, away from Round Mountain. The attitude of these units is presumably due to the tumescence or upwarping caused by the initial endogenous phase of Round Mountain.

Early Phase of Stage 4

Initial growth during this phase of development was endogenous and was caused by the continued upwelling of rhyolitic magma from a vent in the southern portion of the map area. Continued expansion of the dome caused the cooled, solidified outer surface to crack and crumble as its streching limit was exceeded (Macdonald, 1972). Blocks generated by the cracking then fell from the top of the expanding dome to form a crumble breccia around the base. Furthermore whenever expansion cracks on the dome opened, hot viscous magma was extruded resulting in massive breccia units where the lava incorporated blocks of crumble breccia (Macdonald, 1972).

Following the development of the breccia unit in the southern portion of the study area, a minor phase of exogenous activity took place. This involved the eruption of thinly laminated rhyolite flows and the formation of Vivian dome.

Vivian dome (figure 30) is located in the southern part of the Round Mountain volcanic field approximately one mile due south of Andrus dome. The exogenous nature of Vivian dome is exhibited by successive flows that drape over the sides of this construct. The origin of these flows can be traced to a source vent located near the summit of the dome.

Late Phase of Stage 4

Following the eruption of the Vivian rhyolite, the volcanic activity shifted northward to the Round Mountain site. This phase was also endogenous and similar to the endogenous development of the early phase at Vivian dome. A rhyolite breccia (figure 27) virtually identical to the breccia unit in the southern part of the map area was formed during endogeous growth of Round Mountain. This endogenous dome development is believed to have caused the earlier formed rhyolite units adjacent to Round Mountain to dip slightly to the south. The Round Mountain rhyolite breccia unit is approximately 75-90 m thick and is present

circumscribing the Round Mountain dome as the lower slope former.

Textures of both the matrix and the clasts, show extreme horizontal and vertical variation throughout this unit. The breccia clasts are generally angular to subangular and highly devitrified. Sizes of the breccia fragments generally decrease with increased distance from the source vent, ranging from approximately 1.5 meters to less than a centimeter.

Stage 5

Further development of the Round Mountain dome involved a change in the predominant eruptive character from endogenous to exogenous. During this exogenous volcanic phase (figure 28), successive flows of rhyolite were erupted from a vent located near the summit of the dome (figure 31). Macdonald (1972) points out that a majority, if not all, of rhyolitic domes which exhibit late stage exogenous behavior begin with an inital endogenous phase.

There were 3 major rhyolite flows erupted during the early development of this volcanic stage that spread laterally over the dome, and thus smoothed the profile. Based on textures and color, the flows have been mapped, from younger to older, as (1) gray rhyolite, (2) massive gray rhyolite, and (3) buff rhyolite. The exposure of these

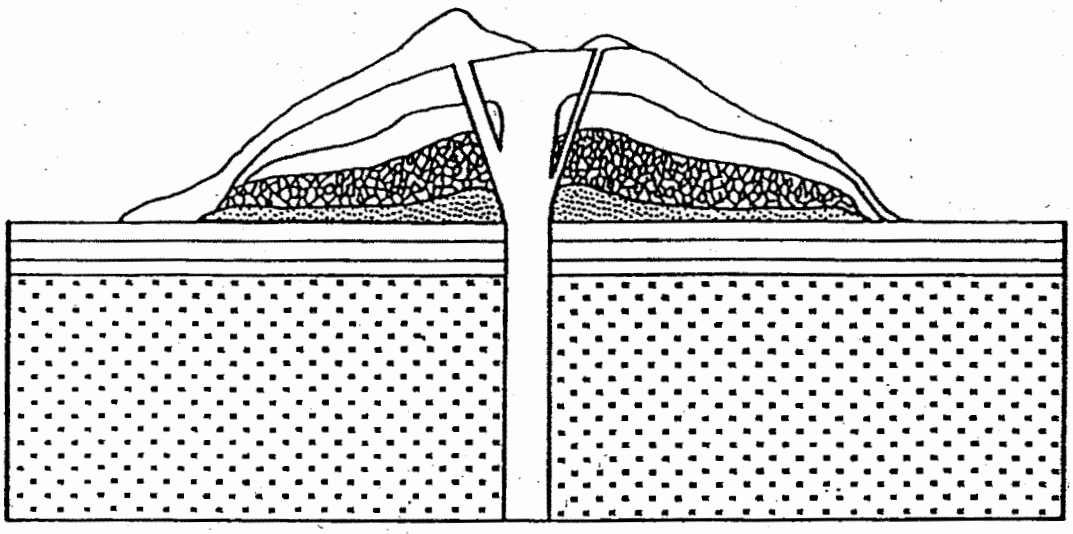

Figure 28 - (STAGE 5) Growth style becomes exogenous with successive rhyolite flows that spread laterally. A late stage dome develops on the southwest side of Round Mtn. showing a preferential southward flow direction.

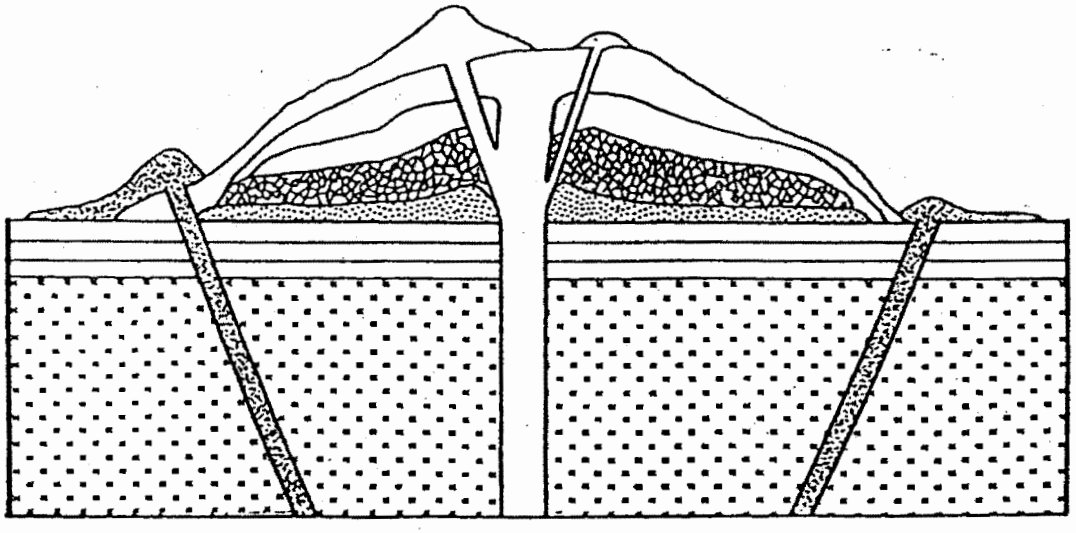

Figure 29 - (STAGE 6) Basaltic dikes intrude the rhyolite flows along the southeast, southwest, and north sides of Round Mtn., forming domes and cinder cones.

Figure 30 - Vivian dome (distant center) showing a smooth profile due to thinly laminated rhyolite flows. Approximately 1 km across photograph.

Figure 31 - Concentric rhyolite pulse flows near source vent at the summit of Round Mountain.

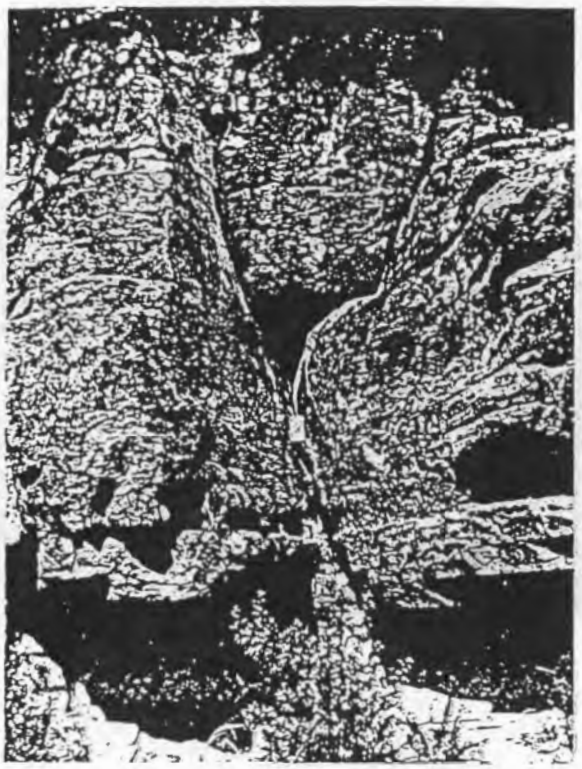

Figure 32 - Polygonal weathering character of the cliff forming massive gray rhyolite unit (Tmgr), east side of Round Mountain.

Figure 33 - Major cliff forming rhyolite flow unit (Tmgr) showing changes in flow thickness on the east side of Round Mountain.

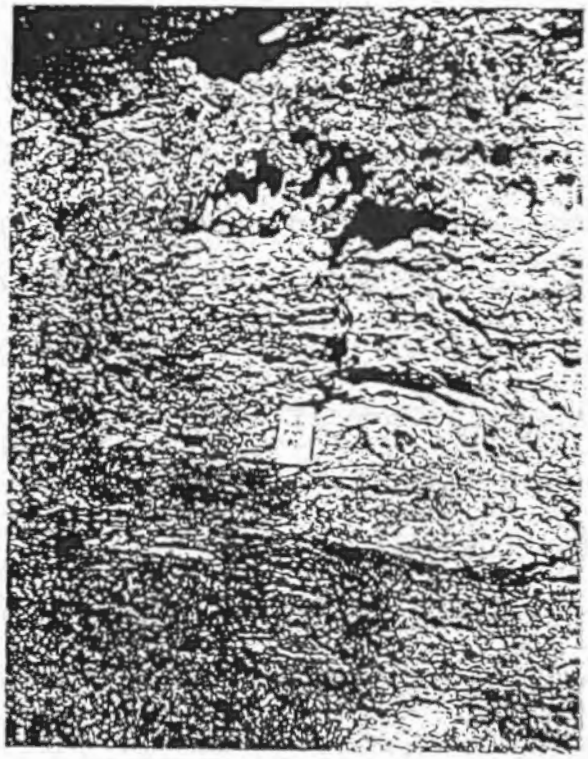

Figure 34 - Interface between the gray (Tgr) and massive gray (Tmgr) rhyolite flows showing mixing and minor brecciation textures, east side of Round Mountain.

Figure 35 - Small intrusion of Andrus rhyolite (Tar) into a cavity on the upper flow surface of the massive gray rhyolite (Tmgr).

flows is confined to the Round Mountain dome. The limited lateral extent of these units infer high viscosity and low volume. This is supported by the fact that the gray and massive gray rhyolite (figure 32) flows are thick, cliff forming units (figure 33). Within these flows there is evidence for the presence of more fluid lava phases locally which are characterized by laminar flow structures on the scale of a hand specimen.

Relative timing of these flows can be defined by examining the contacts between them. Using this method, it was determined that there was little or no elapsed time between the gray rhyolite flow and the older massive gray rhyolite flow. This can readily be demonstrated in the field by evidence of viscous mixing at the interface between the two flows with only minor brecciation (figure 34). The relative time span between the emplacement of the massive gray rhyolite and the buff rhyolite was however sufficiently long to allow for cooling of the upper surface of the massive gray rhyolite flow. This cooling period resulted in a very distinct, sharp contact between the successive flows.

The late phase of this eruptive stage involved minor dome building on the summit of the Round Mountain dome. Two constructs were formed during this phase; the first was a small rhyolite mound, and the second was a secondary rhyolite dome of moderate size. The moderate sized dome,

designated Andrus dome, exhibits an exogenous character. This dome is located on the southwest end of Round Mountain and forms Round Mountain's highest point of relief.

The Andrus rhyolite flows were relatively fluid (figure 35) compared to the massive gray and gray rhyolite units and exhibit a thinly laminated character. They are very similar in both texture and color to the flows from Vivian dome. The greatest volume of rhyolite from the Andrus dome was directed to the south-southeast and was controlled by the topography at the time of eruption.

Stage 6

The final stage of volcanic development of the Round Mountain field involved the emplacement of basalt resulting in a variety of features including domes, cinder cones, radiating dikes, and some flows (figure 29). All of these late stage basaltic constructs are located in areas which outline the rhyolitic domes and flows. Eichelberger and Gooley (1977) observed that mafic bodies are typically satellitic to silicic centers, in both plutonic and volcanic complexes. Only the basaltic constructs of Josep dome and Williams dome exhibit direct petrologic contact with the rhyolitic volcanics.

The source of these basalts is believed to be the same basaltic magma intrusion which acted as a heat source for

Figure 36 - Cross-cutting dike of Josep basalt (Tjb) through Vivian rhyolite (Tvr), south of Josep dome.

Figure 37 - Josep dome showing a slight conical form due to minor late stage basalt eruption. Approximately .75 km across photograph.

the generation of the rhyolite. The emplacement of these late stage basaltic constructs is limited both in time and in space. In the bimodal assemblages of the Snake River Plain and Yellowstone volcanic fields, basaltic eruptions occurred both prior to and after construct-forming rhyolite eruptions (Eaton et al., 1975). In the Round Mountain volcanic field, both the northern and southern parts, basaltic eruptions were limited to a post rhyolite stage.

The locations of these basaltic constructs appears to be controlled, in part, by fractures, especially in the southern half of the field. The fracture control is reflected by the linear character of the dikes radiating from Williams dome, and by the alignment of constructs associated with the Josep basaltic eruptions. The exact origin of these lineaments is not known, but is presumed to be the product of local structural adjustment due to the removal of rhyolitic magma from subsurface chambers.

The development of the fractures allowed basaltic activity to develop as the rhyolitic activity ceased. Bailey and others (1976) have used the distribution of basaltic vents to determine the position of the active subsurface silicic body by assuming that dense basaltic liquid could not pass through the body.

These basaltic constructs and dikes can be seen intruding various late stage rhyolite flows in the southern sector of the volcanic field. One of these basaltic

features is Josep dome (figure 37). Josep dome rises approximately 90 meters above the surrounding plain. It is connected to two minor constructs, to the north and northwest, by feeder dikes. These two smaller constructs appear to have formed simultaneously as evidenced by interconnecting flows.

In figure 36, a dike of Josep basalt exhibits a crosscuting relationship to a late stage Vivian rhyolite flow. The emplacement of Josep dome caused minor upward displacement of adjacent rhyolite units. This displacement is probably due to pre-eruption tumescence of the immediate surroundings as the basaltic magma pushed up through the rhyolite units. Josep dome development was involved in a minor phase of cinder activity prior to the eruption of the final flows. This cinder phase is recognized by areas of cinder pavement associated with the construct, and also by the incorporation of cinders in some latter basaltic flows.

A distinctive basaltic feature in the southern sector of the Round Mountain volcanic field is the Williams dome. Located just southeast of Round Mountain, Williams dome has a local relief of approximately 55 meters. Williams dome consists primarily of radiating dikes which trend roughly north-south and northeast. These dikes radiate from a central vent located at the summit of the construct. There is a small depression at the summit of Williams dome which is filled dominantly with basaltic cinders indicating a late

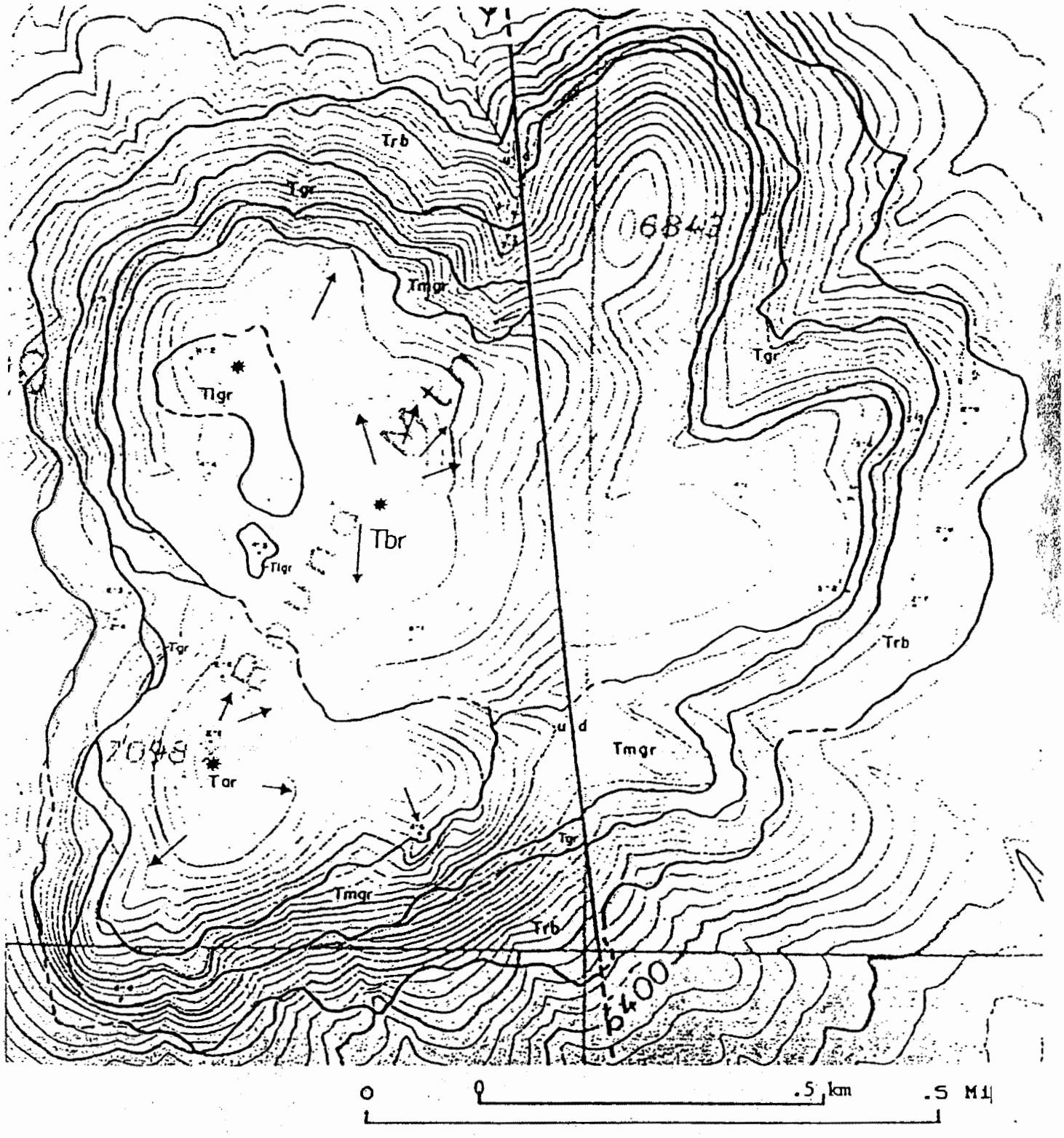

Figure 38 - Geologic map of Round Mountain showing major rotational fault striking N70W. The relative motion is down to the east.

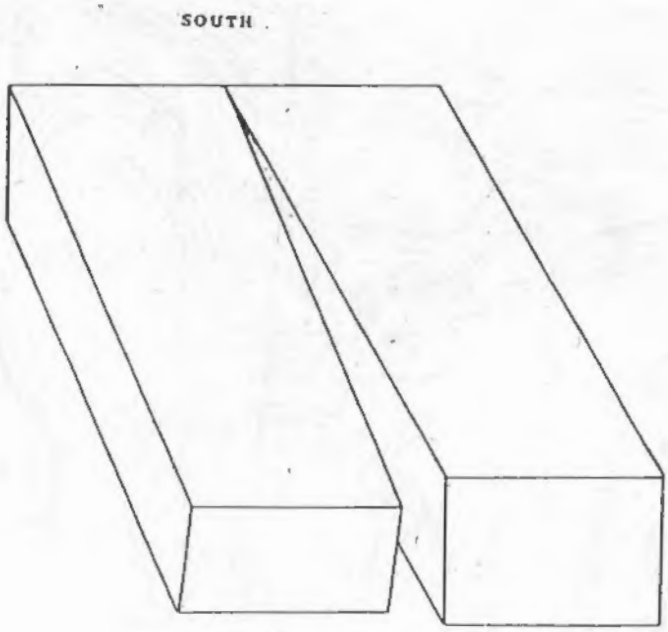

Figure 39 - Block diagram representing rotational or scissor fault relative movement with respect to the faulting of Round Mountain. The downdropped side is to the east with major displacement to the north and relatively zero to the south.

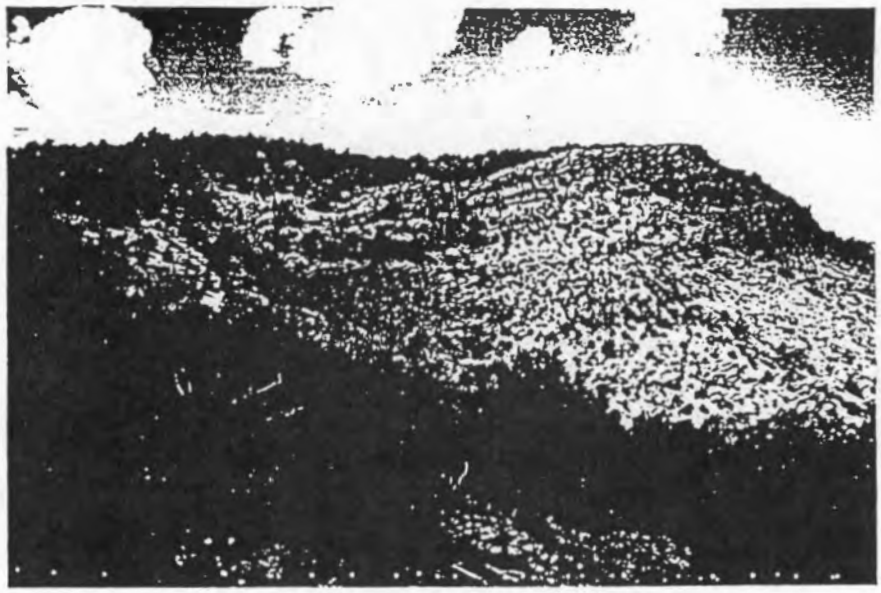

Figure 40 - Rotational fault expressed at the north (looking south) end of Round Mountain. Note truncation of rhyolite flow units to the right. Relative motion is down to the left (east).

stage pyroclastic eruptive phase. The depression is probably due to withdrawal of basaltic magma as volcanic activity slowed and then ceased.

The final phase of development of the Round Mountain volcanic field involved the development of late stage local faults. A major fault strikes approximately N10E directly through the eastern half of Round Mountain (figure 38). This fault scarp which is traceable for just under 2 kilometers. The relative motion is down to the east with relative vertical displacements of 45-55 meters to the north end of Round Mountain (figure 40), and 3-6 meters to the south. These different magnitudes of displacements indicate a rotational, or scissor, fault (figure 39) with its vertex to the south of Round Mountain. Faulting is typically associated with late stage volcanic development when drainage of the underlying magma removes structural support (Macdonald, 1972). Since the location of magma chambers associated with the Round Mountain volcanic activity are controlled by fault zones, it is presumed that the late stage structural adjustments have also occurred along fault zones.

CONCLUSIONS

Round Mountain is a prominent rhyolite dome in northwest Arizona. The dome is approximately 2.1 km in diameter at its base and has a local relief of 268 meters. Round Mountain is centered in a virtual sea of basalt and is late Tertiary in age.

Round Mountain is both endogenous and exogenous in nature. Initial endogenous dome building involved the formation of rhyolite breccia units which constitute approximately 30 to 40 percent of the total erupted rhyolite. Later constructive volcanic phases, mainly exogenous, were characterized by 4 major rhyolite flows which cap the dome.

The Round Mountain volcanic field exhibits strong bimodal characteristics, consisting of high-K rhyolites and alkali olivine basalts. The rhyolites are placed into 10 mappable units based on color and field textures. The basalts are classed into map units on the basis of source vents and flow morphology.

The rhyolites are composed of approximately 90 percent glass with major phenocrystalline phases consisting of sanidine and high-temperature oligoclase.

Emplacement of Round Mountain began with basaltic magma migrating to the upper crust preferentially along deep crustal fracture zones. Rhyolitic magma was generated by

partial melting of a granitic upper crust and later emplaced along surficial fracture zones. The hot basaltic intrusions were responsible for the heat source necessary to initiate partial melting.

REFERENCES CITED

Bailey, R. A., Dalrymple, G. B., and Lanphere, M. A., 1976, Volcanism, Structure, and Geochronology of Long Valley Caldera, Mono County, California, Journal of Geophysical Research, vol. 81, p. 725-744.

Barker,F., 1981, Introduction to special issue on granites and rhyolites : A commentary for the non-specialist, Journal of Geophysical Research, vol. 86, no. B11, p. 10131-10135.

Best, M. G., and Brimhall, W. H., 1974, Late Cenozoic basaltic magmas in the western Colorado Plateaus and the Basin and Range transition zone, U.S.A., and their bearing on mantle dynamics, Geological Society of America Bulletin, vol. 85, p. 1677-1690.

Blake, D. H., Elwell, R. W. D., Gibson, I. L., Skelhorn, R. R., and Walker, G. P. L., 1965, Some relationships resulting from the intimate association of acid and basic magmas, Quarterly Journal of the Geological Society of London, vol. 121, p. 31-50.

Breed, J. B., and Roat, E. C., 1974, Geology of the Grand Canyon, Museum of Northern Arizona, Flagstaff, Arizona, 185 p.

Carr, M.H., Saunders, R.S., Strom, R.G., and Wilhelms, D.E., 1984, The geology of the terrestrial planets, NASA SP-469, p. 107-269.

Carr, M. H., 1980, The geology of Mars, American Scientist, vol. 68, p. 626-635.

Carr, M. H., and Scott, D. H., 1978, Geologic map of Mars, Preliminary version, U.S. Geological Survey.

Carr, M. H., Greeley, R., Blasius, K. R., Guest, J. E., and Murray, J. B., 1977, Some Martian volcanic features as viewed from the Viking orbiters, Journal of Geophysical Research, vol. 82, no. 28, p.3985-4014.

Christiansen, R. L., and Lipman, P. W., 1972, Cenozoic volcanism and plate tectonic evolution of the western United States, pt. 2, Late Cenozoic, Royal Society of London Transactions, vol. 271, p. 249-284.

Cox, K. G., Bell, J. D., and Pankhurst, R. J., 1984, The Interpretation of Igneous Rocks, Allen and Unwin publ., 450 p..

Damon, P. E., 1971, The relationship between Late Cenozoic volcanism and tectonism and orogenic-epirogenic periodicity, in The late Cenozoic glacial ages, Yale University Press, p. 15-35.

Damon, P. E., Shafiqullah, M., and Leventhal, J. S., K-Ar chronology for the San Francisco volcanic field and rate of erosion of the Little Colorado River, in Geology of northern Arizona, in Pt. 1 - Regional Studies, Geological Society of America Rocky Mountain Section Meetings, p. 221-235.

Eastwood, R. L., 1974, Cenozoic volcanism and tectonism of the southern Colorado Plateau, in Geology of northern Arizona, in Pt. 1 - Regional Studies, Geological Society of America Rocky Mountain Section Meetings, p.236-256.

Eichelberger, J. C., and Gooley, R., 1977, Evolution of silicic magma chambers and their relationship to basaltic volcanism, American Geophysical Union Monograph 20, p. 57-77.

Gast, P. W., 1968, Trace element fractionation and the origin of tholeiitic and alkaline magma types, Geochemica et Cosmochemica Acta, vol. 32, p. 1057-1086.

Greeley, R., and Spudis, P., 1981, Volcanism on Mars, Reviews of Geophysics and Space Physics, vol. 19, no. 1, p. 13-41.

Head, J.W., and Gifford, A., 1980, Lunar mare domes : Classification and modes of origin, Moon Planets, vol. 22, p. 235-258.

Heinrich, E. W., 1965, Microscopic Identification of Minerals, McGraw-Hill Book Co., New York, 414 p..

Hereford, R., 1975, Chino Valley formation (Cambrian ?) in northwestern Arizona, Geological Society of America Bulletin, vol. 86, p. 677-682.

Hodges, C.A., 1979, Some lesser volcanic provinces on Mars, NASA Technical Memorandum 80339, p. 247-249.

Hunt, C. B., 1956, Cenozoic geology of the Colorado Plateau, U.S. Geologiacl Survey Professional Paper 279, 99 p.

Irvine, T. N., and Baragar, W. R. A., 1971, A guide to the chemical classification of the common volcanic rocks,

Canadian Journal of Earth Sciences, vol. 8, p. 523-548.

Julian, B. R., 1970, Regional variations in the upper mantle structure in north America, Transactions of American Geophysical Union, vol. 51, p. 359.

Keller, G. R., Braile, L. W., and Schlue, J. W., 1979, Regional crustal structure of the Rio Grande rift from surface wave dispersion measurements, In: Rio Grande Rift : Tectonics and Magmatism, American Geophysical Union, Washington D.C., 438 p..

Lachenbruch, A. H., Sass, J. H., Munroe, R. J., and Moses, T. H., 1976, Geothermal Setting and Simple Heat Conduction Models for the Long Valley Caldera, Journal of Geophysical Research, vol. 81, p. 769-784.

Laughlin, A. W., Brookins, D. G., and Carden, J. R., 1972, Variations in the strontium ratios of a single basalt flow, Earth and Planetary Science Letters, vol. 14, p. 79-82.

Leeman, W. P., 1974, Late Cenezoic alkali-rich basalt from the western Grand Canyon area, Utah and Arizona, isotopic composition of strontium, Geological Society of America Bulletin, vol. 85, p. 1658-1655.

Leonardi, P., 1976, Volcanoes and Impact Craters on the Moon and Mars, Elsevier Publ., p. 225-244.

Lucchitta, I., 1974, Structural evolution of northwest Arizona and its relation to adjacent Basin and Range province structures, in Geology of northern Arizona, in Pt. 1 - Regional Studies, Geological Society of America Rocky Mountain Section Meetings, p. 336-354.

Macdonald, G. A., 1972, Volcanoes, Prentice-Hall Publ., p. 510.

MacDonald, G. A., 1968, Composition and origin of Hawaiin lavas, Geological Society of America Memoir 116, p. 477-522.

McKee, E. D, and McKee, E. H., 1972, Pliocene uplift of the Grand Canyon region, time of drainage adjustment, Geological Society of America Bulletin, vol. 83, p. 1923-1932.

Miyashiro, A., 1975, Volcanic rock series and tectonic setting, Annual Reviews Earth and Planetary Sciences, vol. 3, p. 251-269.

Moore, R. B., Wolfe, E. W., and Ulrich, G. E., 1976, Volcanic rocks of the eastern and northern parts of the San Francisco volcanic field, Arizona: Journal of Research, U. S. Geological Survey, vol. 4, p. 549-560.

Moore, R. B., Wolfe, E. W., and Ulrich, G. E., 1974, Geology of the eastern and northern parts of the San Francisco volcanic field, Arizona: in Geology of Arizona, Pt. II - Area studies and field guides: Geological Society of America Rocky Mountain Section Meetings, p. 465-494.

Moore, R. B., 1973, Alkali-rich, high-alumina basalt from the San Francisco volcanic field, Arizona, Geological Society of America Abstracts with Programs, vol. 5, no. 7, p. 744.

Nealey, David L., 1980, Geology of Mount Floyd and vicintity - Coconino county, Arizona, Northern Arizona University, M.S. thesis, p. 144.

Parsons, W. H., 1969, Criteria for the Recognition of of Volcanic Breccias: Review, Geological Society of America Memoir 115, p. 263-304.

Poldervaart, A., 1950, Correlation of physical properties and chemical composition in the plagioclase, olivine, and orthopyroxene series, American Mineralogist, vol. 35, p. 1067-1079.

Roy, R. F., Decker, E. R., Blackwell, D. D., and Birch, F., 1968, Heat flow in the United States, Journal of Geophysical Research, vol. 73, p. 5207-5221.

Sauck, W. A., and Sumner, J. S., 1971, Residual aeromagnetic map of Arizona, Tucson, Arizona, University of Arizona.

Shoemaker, E. M., Squires, R. L., and Abrams, M. J., 1974, The Bright Angel and Mesa Butte fault systems of northern Arizona, in Geology of northern Arizona, in Pt. 1 - Regional Studies, Geological Society of America Rocky Mountain Section Meetings, p. 355-387.

Shuey, R, T., Schellinger, D. K., Johnson, E. H., and Alley, L. B., 1973, Aeromagnetics and the transition between the Colorado Plateau and the Basin and Range provinces, Geology, vol. 1, no. 3, p. 107-110.

Smiley, T. L., 1958, The geology and dating of Sunset Crater, Flagstaff, Arizona, in New Mexico Geological Society Guidebook 9th Field Conference, Black Mesa

Basin, northeastern Arizona, p. 186-190.

Toulmin, P., Baird, A. K., Clark, B. C., Keil, K., Rose, H. J., Christian, R. P., Evans, P. H., and Kelliher, W. C., 1977, Geochemical and Mineralogical Interpretation of the Viking Inorganic Chemical Results, Journal of Geophysical Research, vol. 82, p. 4625-4634.

Wenrich-Verbeek, K., and Thornton, C. D., 1974, Preliminary geochemical study of the lava flows of the San Francisco Peaks, In: Geology of northern Arizona, in Pt. 2 - Area Studies and Field Guide, Geological Society of America Rocky Mountain Section Meetings, p. 592-601.

Wise, D. U., Golombek, M. P., and McGill, G. E., 1979, Tharsis Province of Mars: Geologic Sequence, Geometry, and a Deformation Mechanism, ICARUS, vol. 38, p. 456-472.

Yoder, H. S., 1973, Contemporaneous basaltic and rhyolitic magmas, American Minerologist, vol. 58, p. 153-17.

Yoder, H.S., and Tilley, C. E., 1962, Origin of basaltic magmas: An experimental study of natural and synthetic rocks systems, Journal of Petrology, vol. 3, p. 792-805.

Young, R. A., 1982, Paleogeomorphic evidence for the structural history of the Colorado Margin in western Arizona, In: Mesozoic-Cenozoic tectonic evolution of the Colorado River region, Californa, Arizona, and Nevada, Frost, E. G., and Martin, D. L. eds., Cordilleran publ., San Diego, California, p. 29-39.

Young, R. A., McKee, E. H., 1978, Early and middle Cenozoic drainage and erosion in west-central Arizona, Geological Society of America Bulletin, vol. 89, p. 1745-1750.